Ph.D. Dissertation of Natural Science

Dual functions of the perirhinal cortex in both perception and memory for objects

사물기억과 지각에 대한 후각주위피질의 역할

February 2017

Graduate School of Natural Science

Seoul National University

Brain and Cognitive Sciences Major

Jae-Rong Ahn

Dual functions of the perirhinal cortex in both perception and memory for objects

Inah Lee

Submitting a Ph.D. Dissertation of Natural Science

February 2017

Graduate School of Natural Science

Seoul National University

Brain and Cognitive Sciences Major

Jae-Rong Ahn

Confirming the Ph.D. Dissertation written by

Jae-Rong Ahn

February 2017

Chair	이 춘 길	(Seal)
Vice Chair	이 인 아	(Seal)
Examiner	정 민 환	(Seal)
Examiner	이 석 호	(Seal)
Examiner	이 준 열	(Seal)

Abstract

Animals including humans guide their actions (e.g., where to go) based on a critical stimulus (e.g., object) in an environment, and can do so even when the stimulus is no longer present owing to the memory of the stimulus. The capability of processing, and recognizing a stimulus for informing prospective behaviors is fundamental to an organism's survival. Since Scoville and Milner's characterization of patient H.M., who demonstrated severe recognition memory deficits following damage to the medial temporal lobe, the perirhinal cortex (PER) has been extensively studied as one of the key neural substrates for object recognition memory.

Two dominant hypotheses have been prevalent in neuroscience regarding the role of the PER. The first hypothesis is that the PER is important for object recognition memory, as has long been acknowledged by human patients, and animal models. The second hypothesis is relatively a recent one and it suggests that the PER involvement in object recognition occurs not only during object memory but also during perceiving object especially when ambiguous objects that share many visual features need to be discriminated.

The functional role of the PER has built primarily on behavioral findings using animal models in which behavioral deficits were found in object memory paradigms following focalized damages to the PER. While more direct evidence may be obtained by recording neural signals, only a handful of physiological studies have been conducted so far to measure neural correlates for objects in the PER. Also, in those studies, recordings were made from animals whose physical body movements were severely restrained, or in tasks that were difficult to correlate neural firings to an object due to multiple confounding factors.

The present thesis is focused on providing physiological evidence that may help fill the gap that remained in the field for decades. In the thesis, I will present a novel object memory paradigm that was designed to address key issues related to object information

processing in the rodent PER. Building on the previous anatomical, behavioral findings on the PER, I sought to address whether (i) the rodent PER neurons would show differential firing patterns for object identities, and (ii) the PER neuronal firings would be modulated by the perceptual features of an object that contains significant feature ambiguity.

Keyword: perirhinal cortex, recognition memory, object memory, object perception
Student number: 2010-24023

Table of Contents

List of Figures

List of Tables

Background and Hypothesis

Background

1. Recognition memory and the medial temporal lobe

Recognition refers to the ability to judge a prior occurrence of a stimulus. It is essentially a matching process whereby a “stimulus out there” is evaluated against the internal representation of the stimulus stored in our memory. Recognition memory is a crucial component of declarative form of memory, and is known to rely on the integrity of the medial temporal lobe (MTL). Recognition memory is independent of other forms of memory such as procedural memory for habits and skills, which is known to recruit the cerebellum or striatum (Squire and Zola-Morgan, 1991). Human patients, such as H.M., who had removed a large portion of the MTL following epilepsy, exhibited a limited form of retrograde and severe anterograde amnesia for recognition memory while the ability to learn and retain motor skills was largely spared (Scoville and Milner, 1957).

Recognition takes place on different types of information such as an item, or spatial location where the item was placed. For some time, it has been believed that the hippocampus and its associated areas in the MTL as a whole make unitary contribution to recognition memory(Squire and Zola-Morgan, 1991; Eichenbaum et al., 1994). A number of studies that employed focalized lesion techniques in animal models, however, have revealed a substantial division of labors across the subregions of MTL (Ennaceur et al., 1996a; Aggleton and Brown, 1999; Bussey et al., 1999).

2. The role of the PER in object recognition memory

A prominent functional dissociation within the MTL with respect to recognition memory was found between the hippocampus and the perirhinal cortex (PER). Lesions restricted to the hippocampus produced severe impairment in spatial memory, but only mild effects on object recognition memory (Ennaceur et al., 1996a; Aggleton et al., 1997; Ennaceur and Aggleton, 1997). Conversely, PER damage yielded deficits specific to object recognition while sparing spatial memory (Ennaceur et al., 1996a; Bussey et al., 1999). A recent study that conducted histological examination of the H.M.'s brain also offered a surprising result that the hippocampus in his brain was largely intact (Annese et al., 2014). This raises the possibility that the recognition memory deficits previously ascribed to the hippocampus may in fact have arisen from other corticles in the MTL areas such as the PER.

While a controversy still exists as to the extent to which the hippocampus and the PER contributes to recognition memory, an emerging consensus is that the PER is involved in recognizing a single item stimulus such as an object while the hippocampus is more engaged when spatial, contextual details surrounding the object needs to be processed(Ennaceur et al., 1996b; Bussey et al., 1999).

The above behavioral findings accord well with the notion the MTL is hierarchically organized into dual information stream: one specialized for nonspatial, object information, and other for visuo-spatial information, respectively (Burwell, 2000; Hargreaves et al., 2005; Eichenbaum and Lipton, 2008; Henriksen et al., 2010). Under this view, the PER is a key area of the nonspatial pathway that provides object-related information to the hippocampus via the lateral entorhinal cortex, as opposed to the postrhinal cortex(POR) that provides contextual, visual scene information to the hippocampus via the medial entorhinal cortex.

Object recognition in animals has widely been tested using the delayed matching-to-sample (DMS), or nonmatching-to-sample (DNMS) paradigm. On each trial, an animal is presented with a sample object, and displaces the object for reward. After a delay during which the object is hidden from view, the animal is presented again with the

same object along with a new object. The animal is then required to displace the sampled object in the DMS (or non-sampled object in the DNMS) task to obtain reward. Animals with lesions in the PER exhibited significant impairment in this task, and the deficit worsened as the temporal delay was prolonged between the sample and test, or as the number of objects to be remembered increased (Meunier et al., 1993; Suzuki et al., 1993; Eacott et al., 1994).

The paradigm, however, has been extensively used for primate research (Meunier et al., 1993; Suzuki et al., 1993; Eacott et al., 1994), but rarely in rodents (Mumby et al., 1990; Mumby and Pinel, 1994), due to the difficulty of implementing the matching or non-matching rule, and a lengthy training protocol required to teach a large number of stimuli to rats (Herremans et al., 1995). To overcome this pitfall, a rodent version of the DMS task was designed by Ennaceur and Delacour, and has since gained widespread popularity among researchers probing rodent object recognition memory (Ennaceur and Delacour, 1988). In a paradigm called the spontaneous object recognition task (SOR), rats initially explore an object affixed in an environment, and after a variable delay, the same object is presented alongside a novel object. The SOR capitalizes on the rat's innate tendency to prefer novel objects, and the relative time the rat spent on exploring the familiar and novel objects is used as a proxy for the memory of the object. Normal rats tend to spend more time exploring the novel object rather than the familiar one, but rats with PER lesions exhibit an equal amount of exploration of the two objects once a sufficient delay (up to 15 minutes) is imposed between initial sampling and later exploration (Ennaceur and Aggleton, 1997; Winters et al., 2004; Winters and Bussey, 2005).

Neurophysiological recordings have been made in the PER to find neural correlates for object recognition memory. In those studies, monkeys were shown a visual stimulus via a monitor screen, and the unit response toward a stimulus decreased as the same stimulus was viewed repeatedly (Miller et al., 1991; Fahy et al., 1993; Xiang and Brown, 1998). The effect of "response decrement" was taken as neural evidence that the PER supports object recognition at the neuronal level. PER neurons also discriminated

between different visual object stimuli, developing an optimal response toward a particular stimulus, as well as toward its paired-associate stimulus (Sakai and Miyashita, 1991; Naya et al., 2001; Naya et al., 2003; Naya and Suzuki, 2011).

Compared to primate research, relatively few studies have been conducted to measure cell activities in the rodent PER. In Zhu et al., PER neurons were recorded while a rat passively viewed a 3-dimensional object (Zhu et al., 1995). The neuronal response in the PER decreased following a repeat presentation of the same object, paralling the results from primate studies. Others recorded PER neurons while rats freely explored objects in an environment (Burke et al., 2012; Deshmukh et al., 2012; Burke et al., 2014). A proportion of PER neurons significantly altered the firing rates in the vicinity of the stimulus objects, forming a so-called “object field” (Burke et al., 2012; Deshmukh et al., 2012), and the fields tended to be maintained over a temporal delay (Burke et al., 2014).

3. The role of the PER in object perception

For an object to be remembered, and recognized later, it first needs to be perceived properly. While traditional theories regarding the role of the PER has focused on the "mnemonic" aspects of the object information processing, a relatively recent hypothesis suggested that the PER also plays crucial a role in object perception when the object has significant "perceptual ambiguity." The theory finds relevance from the anatomical position of the PER. While the PER has long been recognized as a part of the medial temporal lobe, it can also be viewed as an endpoint of the ventral visual pathway extending from the visual cortex and the inferior temporal area TE (Bussey and Saksida, 2002; Naya et al., 2003; Murray et al., 2007; Cowell et al., 2010; Naya and Suzuki, 2011; Kravitz et al., 2013). In addition, multiple sensory inputs including vision, olfaction, audition, and somatosensation, converge on the PER, making an ideal site for high-level sensory integration (Burwell, 2000; Kealy and Commins, 2011). The hierarchical nature of the PER implicates that a more conjunctive representation of an object may be formed in the PER by using elemental sensory features passed down from its upstream cortical areas (Bussey and Saksida, 2002; Naya et al., 2003; Murray et al., 2007; Naya and Suzuki, 2011; Kravitz et al., 2013).

The behavioral evidence that support the perceptual role of the PER has mostly been obtained using concurrent discrimination paradigms. On a given trial, a pair of visual stimuli (target and foil) are presented side by side, and reward is given when the animal chooses the target stimulus (Gaffan and Eacott, 1995; Buckley and Gaffan, 1998b; Buckley et al., 2001; Clark et al., 2011). PER-lesioned animals showed normal discriminability if the rewarded target and non-reward foil were perceptually distinct, but a severe deficit was observed when the two stimuli were perceptually ambiguous (Bussey et al., 2002b; Lee et al., 2005; Bussey et al., 2006; Murray et al., 2007).

The issue has been, however, highly polarized between two academic camps, one supporting the involvement of the PER in perception (when ambiguity exists in objects) and the other implicating the PER in memory only (Baxter, 2009; Suzuki, 2009; Suzuki and Baxter, 2009; McTighe et al., 2010; Clark et al., 2011). The group that rejects

the perceptual role of the PER attribute the deficits in high ambiguity conditions to impaired learning and memory rather than impaired perception. According to them, the impairment can be more related to the failure to maintain the complex stimulus in memory while the animal moved back and forth to compare across the stimulus with overlapping features (Buckley and Gaffan, 2006; Clark et al., 2011).

While the debate has been ongoing for some time, it still remains unsettled without significant conceptual advancement, largely because the issues have been addressed based on behavioral findings, and there have been no physiological recording studies that rigorously dissociated between perception and memory in object information processing.

4. Limitations of the previous rodent object memory paradigms for neurophysiological research

The majority of the single-unit recordings from the PER cell have been conducted in primates. In those studies, visual stimuli are presented to a body-restraint monkey via a monitor screen, and choice is indicated by a hand-held bar, or saccadic eye movement (Miyashita and Chang, 1988; Miller et al., 1991; Liu and Richmond, 2000; Naya et al., 2001; Naya et al., 2003). The first physiological recordings of the rodent PER were made by Zhu and colleagues by emulating this head-fix procedure in primate studies. In a passive viewing paradigm (Zhu et al., 1995), a rat was trained to nose-poke into a hole in a box, and hold the position for a while until an object stimulus in the box became light-illuminated, and visible to the rat. While the head-fix procedure offered an advantage that the animal could be tested in a controlled fashion, it was far from the real-life settings that objects are explored by rats.

To measure object signals in a more naturalistic condition, some researchers turned to the SOR. Since the SOR does not require any training, and the experiment could be set up quite easily, the paradigm has been readily adopted for electrophysiological recordings in the PER (Burke et al., 2012; Deshmukh et al., 2012; Burke et al., 2014). When the PER neurons were recorded while rats foraged in the presence of objects, a portion of PER neurons significantly altered their firing rates in the vicinity of the objects, forming an "object field." While the results seemingly lend support for the PER role in object recognition, the paradigm has several limitations for use in neural recordings. Firstly, it is impossible to determine the exact time point at which the animal initiates and terminates the exploration of an object stimulus, and large variability exists on how exploration is measured across studies (Ameen-Ali et al., 2015). Also, objects are always explored along with its surrounding spatial environments in the SOR, and this makes it difficult to dissociate whether the firing correlates with objects, or the location occupied by the object, or both. More importantly, the memory demand, if any, placed on the task was minimal since the task depends solely on rats' naturalistic behaviors with no

explicit requirement to hold the objects in memory.

Compared to primate research, there has been a lack of consensus on how to test and measure neural signals for objects in rodents. It is probably for this reason that only few studies exist on neurophysiology of the rodent PER, with discrepant results being obtained across studies. PER neurons exhibited the effects of “repetition suppression” when recorded in the paired-viewing paradigm by decreasing firing rates toward a repeated presentation of the same object stimuli (Zhu et al., 1995). However, the effects were not so clearly visible in the free exploration paradigms (Burke et al., 2012; Deshmukh et al., 2012; Burke et al., 2014). A majority of the PER neurons showing object fields near object stimuli did not seem fire in relation to its identities, showing similar response patterns toward different objects (Burke et al., 2012; Deshmukh et al., 2012; Burke et al., 2014).

The neurophysiological investigation of the PER with respect to object perception has equally suffered a lack of proper behavioral designs. Most of prior animal studies probing object perception utilized concurrent discrimination paradigms where a choice had to be made while viewing multiple objects presented simultaneously (Bussey et al., 2002b; Lee et al., 2005; Bussey et al., 2006; Murray et al., 2007). While viable for behavioral research, the paradigm is not adequate for neuronal recordings since it is impossible to measure direct correlation between a neural firing and a stimulus since the stimulus is always presented along with other stimuli.

Hypothesis

In this thesis, I present a novel, goal-directed object memory paradigm that improves upon traditional rodent object recognition tasks such as passive-viewing, the SOR, or concurrent discriminations. In the current paradigm, 2-dimensional digitized object images were used as stimuli so that stimulus sampling was limited to the visual modality only. I preferred to use computer-generated digital object images instead of real-life 3-dimensional objects since it gave me a better control over the onset and offset of the stimuli, and it was easier to manipulate the level of perceptual ambiguity in the objects in a more parametric manner. Stimulus ambiguity was created by using a perceptual morphing method wherein two perceptually distinct images became more and more similar to each other as ambiguity level increased. The morphing was applied to two well-learned standard objects so that no new learning was required, and the memory load at the time of perceptual sampling minimized. To ensure proper stimulus sampling within a restricted time window, I trained rats to directly contact the object image using its snout, and the object was only visible until it being touched. For more direct measurement of object memory, only a single object stimulus appeared per trial, the rat was required to explicitly indicate the memory of the object by choosing a specific target image paired with the object in the absence of the object.

In chapter 1, I tested the feasibility of this paradigm in rats, and also whether the PER is required for this task. I then conducted multi-unit recordings from the PER while rats were actively engaged in the task. Given the previous behavioral findings that the PER is crucial for object recognition memory, I hypothesized that the rodent PER neurons would exhibit differential firing patterns for different object stimuli. The research presented in chapter 1 has been published in Journal of Neuroscience (Ahn & Lee, 2015).

In chapter 2, I put to test the long-held controversy of whether the PER is more important for object perception, or object memory. For the purpose of separating the perceptual and mnemonic cognitive components present in the current design, the event

period (previously defined from object appearance to behavioral choice) was sub-divided into perceptual object sampling period and mnemonic choice period. Given that the perceptual demand was higher in the sampling period, and the mnemonic demand in the choice period, I hypothesized the PER neurons may exhibit differential neural response patterns in accordance with the changing task demand.

Chapter 1. Neural correlates for object-associated choice behavior in rodent perirhinal cortex.

Abstract

The perirhinal cortex (PER) is reportedly important for object recognition memory, with supporting physiological evidence obtained largely from primate studies. Whether neurons in the rodent PER also exhibit similar physiological correlates of object recognition, however, remains to be determined. I recorded single units from the PER in a PER-dependent object memory task in which, when cued by an object image, the rat chose the associated target from two identical discs appearing on a touchscreen monitor. The firing rates of PER neurons were significantly modulated by critical events in the task, such as object sampling and choice response. Neuronal firing in the PER was correlated primarily with the conjunctive relationships between an object and its associated choice response, although some neurons also responded to the choice response alone. However, I rarely observed a PER neuron that represented a specific object exclusively irrespective of spatial response in rats, although the neurons were influenced by the perceptual ambiguity of the object at the population level. Some PER neurons fired maximally after a choice response, and this post-choice feedback signal significantly enhanced the neuronal specificity for the choice response in the subsequent trial. Our findings suggest that neurons in the rat PER may not participate exclusively in object recognition memory, but that their activity may be more dynamically modulated in conjunction with other variables, such as choice response and its outcomes.

Keyword: perirhinal cortex, object recognition, nonspatial memory, spatial memory, choice outcome

Introduction

A theory holds that two functionally distinct information-processing streams exist in the medial temporal lobe: one is specialized in spatial memory and the other in nonspatial memory (Burwell, 2000; Hargreaves et al., 2005; Eichenbaum and Lipton, 2008; Henriksen et al., 2010). According to the theory, spatial information is processed in the postrhinal cortex (POR) and sent to the hippocampus via the medial entorhinal cortex (MEC), whereas nonspatial information is conveyed by the perirhinal cortex (PER) via the lateral entorhinal cortex. In accordance with this theory, many studies have focused on the nonspatial functions of the PER, implying a role for the PER in object recognition memory (Meunier et al., 1993; Ennaceur et al., 1996a; Buckley and Gaffan, 1998a; Winters and Bussey, 2005) and perhaps also in object perception (Bussey et al., 2002; Lee et al., 2005; Murray et al., 2007; Baxter, 2009).

In apparent support of the above viewpoint, studies have reported single units in the PER that responded to particular objects in an object recognition memory task in primates (Brown et al., 1987; Miyashita and Chang, 1988; Liu and Richmond, 2000; Naya et al., 2003). However, previous anatomical studies show that the PER in rodents receives heavy projections from the POR, and the POR reciprocally connects to the MEC (Burwell and Amaral, 1998; Furtak et al., 2007b). Therefore, the PER may process some spatial information in rodents (Liu and Bilkey, 1998; Burke et al., 2012). The PER also receives dense projections from other subcortical structures, including the amygdala, ventral striatum, and ventral tegmental area (Van Hoesen et al., 1981; Pitkanen et al., 2000; Kealy and Commins, 2011). This suggests that reward-related neuromodulatory signals may influence neuronal activity in the PER (Liu et al., 2000; Liu and Richmond, 2000; Mogami and Tanaka, 2006; Clark et al., 2012; Ohyama et al., 2012). Whether the rodent PER also exhibits functionally similar physiological properties remains to be determined.

Only a handful of physiological studies have examined the roles of the PER in object recognition in rodents, although many behavioral studies have explored the impact

of perturbations in the PER (Aggleton et al., 1997; Ennaceur and Aggleton, 1997; Norman and Eacott, 2005). Prior studies examining single-unit activity in the PER primarily used spontaneous object recognition paradigms (Burke et al., 2012; Deshmukh et al., 2012). In those studies, PER neurons exhibited poor spatial firing patterns, but fired in apparent association with objects by changing firing locations when the objects were moved to different locations. It is possible that these "object fields" (Burke et al., 2012; Burke et al., 2014) may be formed and retrieved through interactions between object and spatial information in the PER.

In the present study, I recorded single units simultaneously in the PER while rats performed a paired-associate memory task between objects and spatial choices. I sought to find whether the PER demonstrated neural correlates for specific objects, as shown in primates, or whether neuronal activity in the PER was also influenced by other variables including spatial response and choice outcome.

Materials and methods

Subjects

Four male Long-Evans rats (350-420g at the time of surgery) were used for the study. The animals were housed individually under a 12 h light:dark cycle and all experiments were conducted in the light phase of the cycle. Rats were maintained at 85% of the free-feeding weight throughout the experiment with *ad libitum* access to water. All protocols and procedures conformed to the guidelines in the National Institutes of Health's Guide for the Care and Use of Laboratory Animals and those determined by the Institutional Animal Care and Use Committee at the Seoul National University.

Behavioral Apparatus

Behavioral experiments were performed on an elevated linear track (7×44.5 cm; 84 cm above the floor) with a food tray attached at its end (**Figure 1**). At the other end of the track was a guillotine door-operated start box (16×22.5×30 cm). An array of three LCD monitors was positioned right above the food tray. The center monitor was only used and it was equipped with an infrared touchscreen panel (Elo Touch Systems) to detect animal's touch responses. A transparent acrylic panel with three round holes (diameter = 3 cm) was overlaid on the monitor to define the animal's response areas. Opaque acrylic dividers were installed on both sides of the object to prevent the rats from using a mediating response strategy (Chudasama and Muir, 1997). Four fiber optic sensors (Autonics, Pusan, Korea) were installed along the linear track to record movement. The breakage of the 3rd sensor (installed in front of the monitor) triggered the onset of a gray-scaled object stimulus (4x6 cm) in the monitor. The apparatus was located in a curtained area, and was dimly lit by a halogen light (0.2 lx) on the ceiling. White noise (80 dB) was provided throughout the experiment. A custom-written Matlab software (using PsychToolbox) was used to control the onset and offset of experimental stimuli.

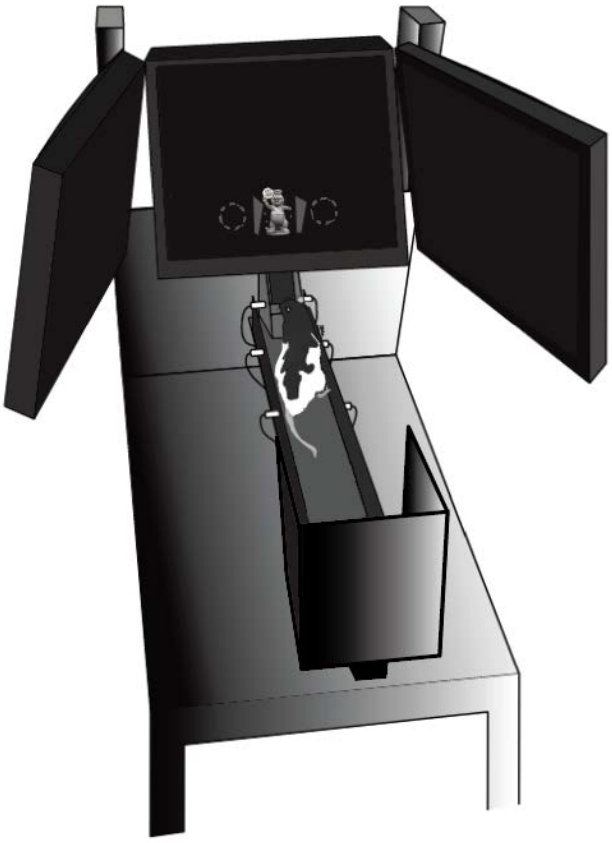

Figure 1. Behavioral testing apparatus A rat was required to nose-poke an object image ("Toy" in this example) presented on a monitor after coming out of a start box and choose one of the response discs (dotted circles) that appeared subsequently following the object offset.

Behavioral paradigm

Rats (n=4) were trained in an object memory task (**Figure 2A**) in which, once a trial started by the opening of the start box, the rat exited the start box and moved toward the end of the track. When the rat activated a fiber optic beam sensor installed in front of the monitor at the end of the track, a cueing object (standard object: Toy or Egg, each occupying a 4 × 6 cm area on the screen) appeared. All objects were adjusted to equal luminance with the following methods. First, objects were adjusted to have equal average gray values in Photoshop. Then, the luminance of object stimuli was measured (and adjusted until showing equal luminance) in an experimental setup by placing a professional lux meter at a fixed distance from the LCD monitor when each stimulus was displayed on the screen. When the animal touched the object with its snout, the object disappeared, a tone sounded (2.25 kHz, 83 dB), and two identical gray response discs (each with a diameter of 3 cm) appeared on both sides of the previous object's location. The rat was required to touch the disc associated with the previously sampled object to obtain a cereal reward (Cocoballs, Kellogg's) in the food tray. When one of the discs was touched, both discs disappeared and the accuracy of the choice was signaled immediately with auditory feedback (1.5 kHz and 150 Hz for correct and error choices, respectively). When the animal made an error, no reward was provided.

Once the rats were trained to criterion (i.e., ≥ 70% correct choices for both objects for two consecutive days) with the standard objects (STD session; **Figure 2B**), they underwent hyperdrive implantation surgeries. After recovery from surgery, rats performed STD sessions during the adjustment of electrodes and were then tested in ambiguity (AMB) sessions in which the standard object images were parametrically morphed into one another using a commercial software product (Morpheus Photo Animator, ACD Systems, Saanichton, Canada) to yield ten different object images (**Figure 2B**). The half of the images that were perceptually closer to the standard Toy object shared the reward contingency of the original stimulus, and the same was true for the standard objects in the Egg category. Each object appeared 12 times, constituting 120 trials in total per session. The reward contingency for object-disc association was

counterbalanced among rats, and the sequence of object stimuli presented across trials was pseudo-randomized with the restriction that the same stimuli did not appear for more than 3 consecutive trials.

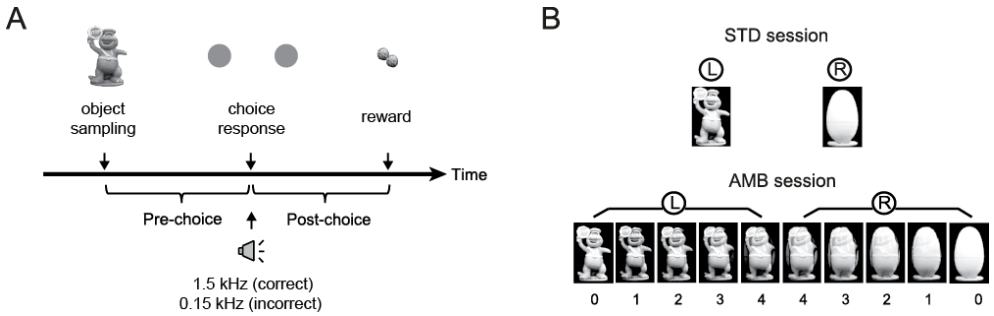

Figure 2. Object memory paradigm (**A**) Schematic illustration of sequential events in a trial (object sampling, choice response, and reward) in the object memory task. Reward was provided only in correct trials. Using the choice moment as a reference, a trial was divided into a pre-choice and a post-choice period. Tones of different frequencies were delivered upon the choice response to offer feedback for the accuracy of the choice. (**B**) Object stimuli used in the task. Two objects (Toy and Egg) were used for standard object (STD) sessions. L and R indicate the correct disc choices associated with the objects. For ambiguity (AMB) sessions, the two original objects were morphed into one another to yield ten different objects. Numbers below the images denote perceptual ambiguity levels (0 to 4 indicating no ambiguity to the highest ambiguity). The rat was required to make a choice response to the morphed object to obtain a reward on the basis of the learned associations between the standard objects and choice discs.

Hyperdrive implantation

A microdrive array (hyperdrive) composed of 16 tetrodes was used for electrophysiological recordings. Platinum-iridium were (17.8 μm in diameter) were twisted and heat-bonded to make a tetrode. The final impedance of the wire was adjusted to 150–300 kΩ (measured in gold solution at 1 kHz with an impedance tester). The hyperdrive was implanted in the right hemisphere by using the following target coordinates for tetrodes: 3.8–4.8 mm posterior to bregma, 6.8 mm lateral to midline, 3–4 mm below the skull surface. For placing the hyperdrive as closely implanted as possible to the PER without damaging unwanted cortical areas, the temporalis muscles on the right side were fully retracted. A hole was drilled on the skull surface, matching the size of the radius of the bundle tip. The drive was lowered down vertically to the target position. The drive was chronically affixed to the skull with eight anchoring screws and bone cement.

Reversible inactivation of the PER

To test whether the PER was required in the OCSC task, I trained a separate group of rats (n = 3) in the same task with only standard objects (STD in **Figure 2B**). After reaching the pre-surgical performance criterion, animals were implanted bilaterally with guide cannulae (23G) coupled with stylets protruding 1 mm from the cannulae tips at the following coordinates: 4.8 mm posterior to bregma, 7.6 mm lateral to midline, 3.9 mm below the skull surface (tips angled at 10° laterally). After recovery from surgery, animals were retrained to criterion, and underwent two experimental sessions. On the first day of testing, phosphate-buffered saline (SAL, 0.5 μL per site) was injected 20 min before testing. On the following day, a GABA-A receptor agonist, muscimol (MUS, 0.5 μg/0.5 μL per site), was injected to temporally inactivate the PER. Fifty trials were given for all testing sessions. After all behavioral experiments, the cannulae positions and the spread of MUS were verified by examining the diffusion range of fluorescent MUS (BODIPY TMR-X muscimol, Invitrogen) under an epifluorescence microscope.

Electrophysiological recording

Neural signals were amplified (1,000–10,000 times) and digitized at 32 kHz (filtered at 300–6,000 Hz) using a Digital Lynx data acquisition system (Neuralynx, Tucson, AZ). Neural signals were relayed through a slip-ring commutator to the data acquisition system. Information about the animal's position and head direction was detected with LEDs attached to the preamplifier connected to the hyperdrive. The LED signals were captured through a ceiling camera and fed to a frame grabber at 30 Hz. To position the tetrodes at target locations, individual tetrodes were lowered daily by small increments for several days during which time the rats experienced only STD sessions. Once the majority of tetrodes reached the PER, spiking activities of single units were recorded in AMB sessions for 4 to 5 days.

Most tetrodes were lowered daily by small increments, and I made no special attempts to hold a single neuron across multiple sessions for the sake of maximizing the number of neurons recorded simultaneously for each day. However, a possibility exists that the same neurons were recorded across several sessions because, occasionally, some tetrodes remained in the same position for days. This issue was examined by comparing the waveform parameters, including spike amplitude (from peak to trough; from peak to baseline), spike width (from peak to trough), and the mean firing rates in every pair of neurons that were recorded from the tetrodes that were not moved across sessions. Among 100 neurons in the PER that were used in the final analyses (for exhibiting significant modulation in firing in association with critical events in the task), only 13 neurons exhibited minimal differences (i.e., identified in the lower 95% confidence limits) in the above parameter distributions for waveforms, and these neurons might have been the same neurons. I found that none of these neurons were recorded for more than three consecutive sessions.

Unit isolation

Single units (n=415) were isolated offline using a cluster-cutting method based

on various waveform parameters, including peak and energy as previously described (Kim et al., 2011). The following set of criteria was subsequently applied to the clustering-based unit isolation results to yield the neurons for further analyses: (a) units with sufficient cluster separation (isolation distance ≥ 10) (Harris et al., 2001) and signal-to-noise ratio (L-ratio < .3) (Schmitzer-Torbert et al., 2005), and (b) task responsiveness (i.e., the average firing rate from object onset to food-tray access > 1 Hz).

Histological verification of electrode position

After the last recording session, small electrical currents (10 μA for 10 s) were passed through individual tetrodes to mark the final tetrode tip locations. Following this, the rat inhaled an overdose of CO2 and was perfused transcardially with 0.1 M phosphate-buffered saline solution, followed by 4% v/v formaldehyde solution. The brain was stored in a sucrose-formalin solution at 4°C until it sank to the bottom of the container. The brain was frozen and sectioned at 30 μm using a sliding microtome. The brain slices were mounted and stained with thionin for Nissl bodies, and the adjacent sections were stained for myelin with a 0.2% buffered gold chloride solution followed by fixation (5 min) in a 2.5% sodium thiosulfate solution. Photomicrographs were taken, and the positions of individual tetrodes were reconstructed based on the histological data and physiological depth profiles recorded during data acquisition.

Data analysis

Behavioral data analysis

The performance of each rat was measured by calculating the proportion of correct trials within a session. A bias index for object category was calculated by subtracting the average performance for the Egg category from that for the Toy category. For each trial, two event epochs were defined using the moment at which a choice response occurred as a reference point, as follows: (i) pre-choice period (from object onset to choice) during which a decision for a choice response was required after sampling an

object cue, and (ii) post-choice period (from choice to food-tray entry) during which auditory feedback signaled the accuracy of the choice, and the rat moved its snout into the food tray (**Figure 2A**).

Raster plots

A raster plot was built by aligning spike timestamps with reference to the timestamp for the choice event (bin size = 50 ms, time window = 4 s before and after choice). Among the cells with mean firing rates exceeding 0.5 Hz in the event period, when the mean firing rate associated with either the pre-choice or the post-choice period was significantly different (t-test, alpha = 0.01) from the baseline firing rate (i.e., mean firing rate for the 1-s period before the object cue appeared), the unit was labeled as event-responsive. Trials with missing timestamps or inter-event latencies exceeding 2 SDs from the mean session latencies were removed from the analyses.

Task-factor analysis and multicollinearity control

Neurons that significantly modulated their activity during the task events were further subjected to a two-way ANOVA with the object category (Toy and Egg) and spatial choice (left and right touch responses) as main factors. If the ANOVA showed significant effects for both factors for a given cell, a multicollinearity problem (i.e., two factors significantly correlated) was suspected, and a control analysis was conducted by determining whether the neuronal firing patterns associated with the correct and error trials were significantly different from each another while holding either the object or the choice factor constant. For example, the trials associated with the Toy category were sorted into correct and error trial types (associated with opposite spatial responses), and the firing-rate distributions for the two trial types were compared with one another (t-test, alpha = 0.05). This procedure was repeated for the Egg category as well by sorting the same trials accordingly. If the firing-rate distributions associated with the correct and incorrect trials for any object category were significantly different from one another, the significance from the ANOVA for the object factor was rejected, and the neuron was

labeled as not showing object selectivity. The same procedure was repeated for the choice factor. These conservative measures conducted in tandem with the ANOVA ensured that only those neurons relatively free from the multicollinearity problem were used for analyses in the current study.

Population rastergram analysis

For analyzing neuronal firing patterns associated with individual objects at the population level, a population rastergram was constructed for each object stimulus by using all the neurons (n = 64) that were active in the pre-choice period (bin size = 200 ms; 12 bins in total based on the mean response latency in the pre-choice period). Each neuron's firing rates in the population rastergram (only correct trials were used) was normalized by the neuron's maximal firing rate, and the individual neuronal rastergrams associated with the STD objects were ordered according to the peak firing locations. The same ordering scheme was used for the AMB objects. The entire population rastergram was then smoothed with a moving average method (window size = 5 bins).

Post-choice peak-firing latency analysis

For the PER neurons that exhibited maximal firing rates during the post-choice period, a trial-by-trial latency of the peak firing was measured separately from the moment of spatial choice and from the food-tray entry event (bin size = 50 ms). The peak-firing rate in a given trial was defined as the firing rate exceeding 2 SDs from the mean firing rate in the 8 s time window centered at the choice event. The trials that did not exhibit a peak based on this criterion and also the cells with peaks emerging outside the post-choice period were excluded from the analyses. The latency histograms were smoothed using a kernel density estimation ($\sigma = 0.18$). The median peak locations were averaged and compared using a Wilcoxon signed-rank test (alpha = 0.05).

Receiver operating characteristic (ROC) analysis and response prediction index (RPI)

The trials were sorted into the following two types based on the choice outcome of the immediately preceding trial: PreT-correct trial (when a correct choice was made in the preceding trial) and PreT-error trial (when an error response was made in the preceding trial). To correct for spurious effects that might arise from different numbers of sample trials in PreT-correct and PreT-error trials, a bootstrapping procedure was conducted by randomly collecting 1,000 samples from the Pre-T correct trials and also from the PreT-error trials as well, and by constructing the firing-rate distributions associated with the touch responses for the left and right discs in the pre-choice period for each trial type. An ROC curve was then plotted based on the two distributions. The size of the area under the curve (AUC) was measured in the ROC plot. These steps were repeated for 1,000 times and the AUC of the ROC curves were averaged to obtain a response prediction index (RPI). The resulting RPI quantified the amount of overlap in the two firing-rate distributions associated with the opposite spatial choice responses, with a higher AUC corresponding to a better prediction for an upcoming behavioral choice given the firing rate of a neuron in the pre-choice period in a given trial. One session was eliminated because of a significant response bias and four units from the session were not used for calculating the RPI. A baseline RPI was computed by averaging the AUCs from 1,000 randomly selected trials irrespective of trial conditions.

Results

The PER is required in the object memory task

I firstly examined how the rats performed in this object memory task. In STD sessions, rats made correct choices in approximately 80% of the trials, and their performance dropped by approximately 10% in AMB sessions ($t_{(3)} = 2.62$, $p = 0.08$, t-test) (**Figure 3A**). In AMB sessions, performance decreased significantly as the level of ambiguity increased ($F_{(4,64)} = 29.68$, $p < 0.0001$, repeated-measures ANOVA) (**Figure 3B**). When object ambiguity was low or moderate (0–2 in **Figure 3B**), rats maintained performance levels similar to those during STD sessions (t values < 2.94, p values > 0.09, Bonferroni-corrected *t*-test, alpha = 0.01). By contrast, performance decreased significantly when ambiguity was relatively high (ambiguity level 3 and 4 in **Figure 3B**), compared with that in the STD condition (t values > 33.03, p values < 0.0001, Bonferroni-corrected t-test). Notably, despite the significant decline in performance, rats still performed significantly at above chance level (50%) in the high ambiguity conditions (t values > 4.41, p values < 0.001, Bonferroni-corrected one-sample t-test, one-tailed) (**Figure 3B**). Except for one rat, all rats developed a slight bias toward a particular object category, but the bias was not statistically significant (**Figure 3C**; sign test for individual animals, p values = n.s.). Furthermore, directions of performance bias varied across rats (**Figure 3D**), suggesting that a particular object stimulus was not preferred to the other innately. Also, the bias cannot be attributed to the rat preferring a particular motor response to one side because, for example, rat 144 was run with an opposite object-response reward contingency compared to rat 141, but both rats showed the performance bias in the same direction (**Figure 3D**). The object bias indices were averaged across animals and plotted as a function of sessions. Overall, no significant bias was found toward a particular object category in any of the sessions ($H = 1.94$, $p = 0.75$, Kruskal-Wallis test) (**Figure 3E**), and no significant improvement in performance was seen across AMB sessions ($F_{(3,9)} = 1.93$, $p = 0.20$, repeated-measures ANOVA) (**Figure 3F**). Rats took

approximately 2.7 s (2.76 ± 0.31; mean ± SEM) on average to touch the choice disc in the pre-choice period and approximately 1.5 s (1.60 ± 0.11; mean ± SEM) to enter the food tray from the moment of disc touch in the post-choice period. The latency did not differ across the ambiguity levels (F values < 1.75, p values > 0.15, repeated-measures ANOVA).

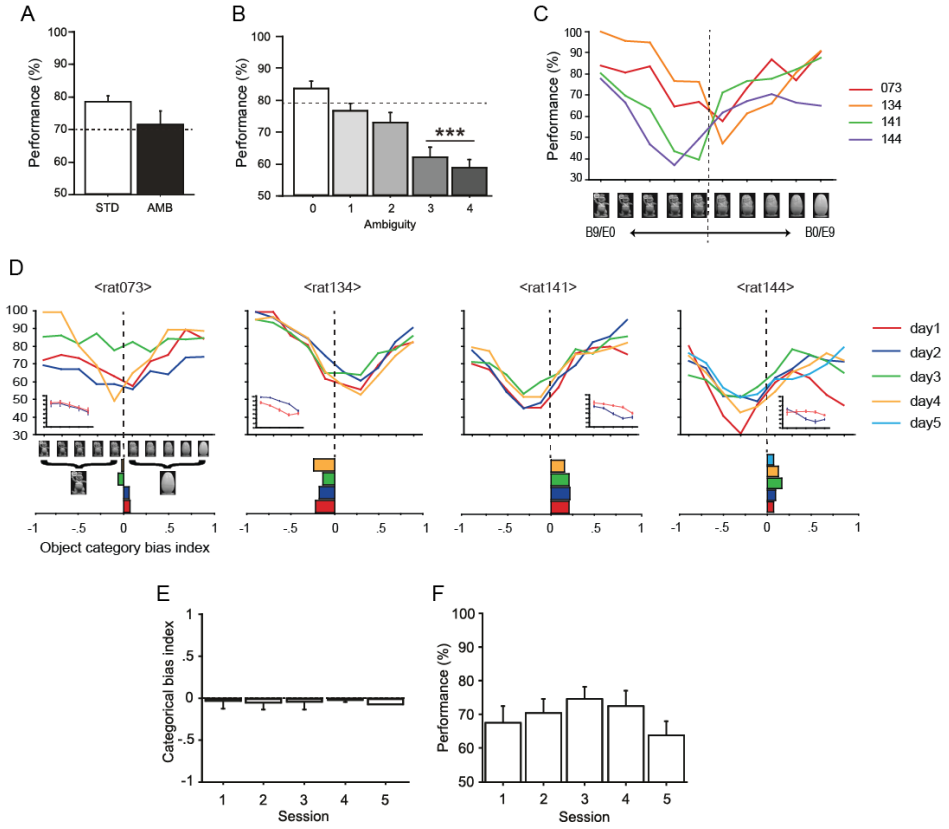

Figure 3. Behavioral performance in the object memory task (**A**) Performance during standard (STD) and ambiguity (AMB) sessions. The performance decreased by approximately 10% in the AMB sessions compared to the STD sessions. Dotted line denotes pre-surgical performance criterion for surgery (70%). (**B**) Performance as a function of ambiguity level (0 lowest, 4 highest). The behavioral performance decreased as the ambiguity level increased. The performance significantly decreased in the high ambiguity conditions (level 3 to 4) compared to the STD session (dotted line). ***$p < 0.0001$. (**C**) Performance curves for individual animals (color-coded). Dotted line denotes choice category border. (**D**) Daily performance curves (moving averaged using a 3-day window) of individual rats. Horizontal bar graphs represent daily performance biases toward particular object categories, calculated by subtracting the performance of Egg category from the performance of Barney category. Zero means no bias. *Inset*: Performance (y-axis) as a function of increasing ambiguity level (0 to 4, x-axis), plotted separately for Toy (blue) and Egg (red). Mean ± s.e.m. (**E**) The object bias indices plotted as a function of task sessions. No significant bias was found toward particular objects in any of the sessions. (**F**) There was no

significant effect of learning across sessions in the AMB sessions. Because only one rat performed on day 5, the analysis was conducted on data obtained from days 1 to 4 only. All graphs show mean ± SEM.

To determine whether the PER played critical roles in the current task, I trained a separate group of animals (n=3) in the STD version of the task and tested in the presence or absence of MUS-induced inactivations in the PER. According to the histological results, the diffusion of the f-MUS seemed largely located in A36 (**Figure 4A**), although one needs to be careful when interpreting the results because the diffusion range of f-MUS might be underestimated compared to that of the standard MUS compound (Allen et al., 2008). Nonetheless, the histological results should not undermine our behavioral findings mainly because visual information is critical in the current task and A36 is known to receive richer visual inputs from upstream visual areas than A35 (Burwell and Amaral, 1998).

A paired *t*-test revealed a significant difference in task performance between SAL and MUS conditions. Rats with SAL injected in the PER performed well (above 80% correct performance), whereas MUS inactivation of the PER significantly decreased performance compared with that in the SAL condition ($t_{(2)} = 4.00$, $p = 0.05$, paired t-test) (**Figure 4B**). When compared to the baseline (one-sample t-test), the performance in the SAL condition was significantly above chance ($t_{(2)} = 27.71$, $p < 0.01$), whereas rats performed near at chance level once MUS was injected ($t_{(2)} = 3.84$, $p = 0.06$) (**Figure 4B**). It is unlikely that nonspecific side effects of MUS caused the performance deficits because response latencies (measured from object onset to choice) in the two drug conditions did not differ significantly ($t_{(2)} = -1.29$, $p = 0.32$, paired t-test).

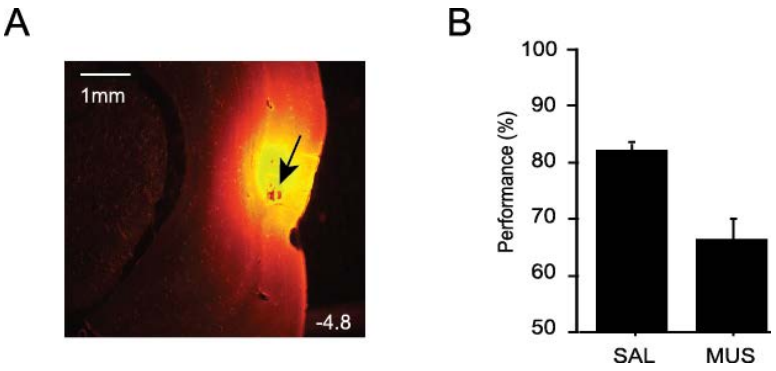

Figure 4. Impairment in performance upon the inactivation of the PER (**A**) A representative photomicrograph of tissue injected with fluorescent muscimol (f-MUS). Note the localized spread of MUS in the PER. The number on the right bottom corner indicates the distance from bregma (mm). (**B**) PER inactivation affected the performance in the OCSC task compared the saline (SAL) injection condition. Mean ± SEM.

Spiking properties of PER neurons

I recorded the activity of single units in the PER while rats were tested in AMB sessions. The electrodes covered the dorsoventral extent of the PER, sampling units from both deep and superficial layers of different subfields (A35 and A36) (**Figure 4A** and **Figure 4B**). Among the PER units that were isolated through the cluster-cutting procedure, one hundred and eleven units survived the quality criteria (see **Materials and methods**), and were analyzed further (**Figure 4C** and **Table 1**). The mean firing rate of the units was 4.58 ± 0.41 Hz (mean ± SEM). Units with high firing rates (> 10 Hz, n = 10) were eliminated from further analysis (Deshmukh and Knierim, 2011).

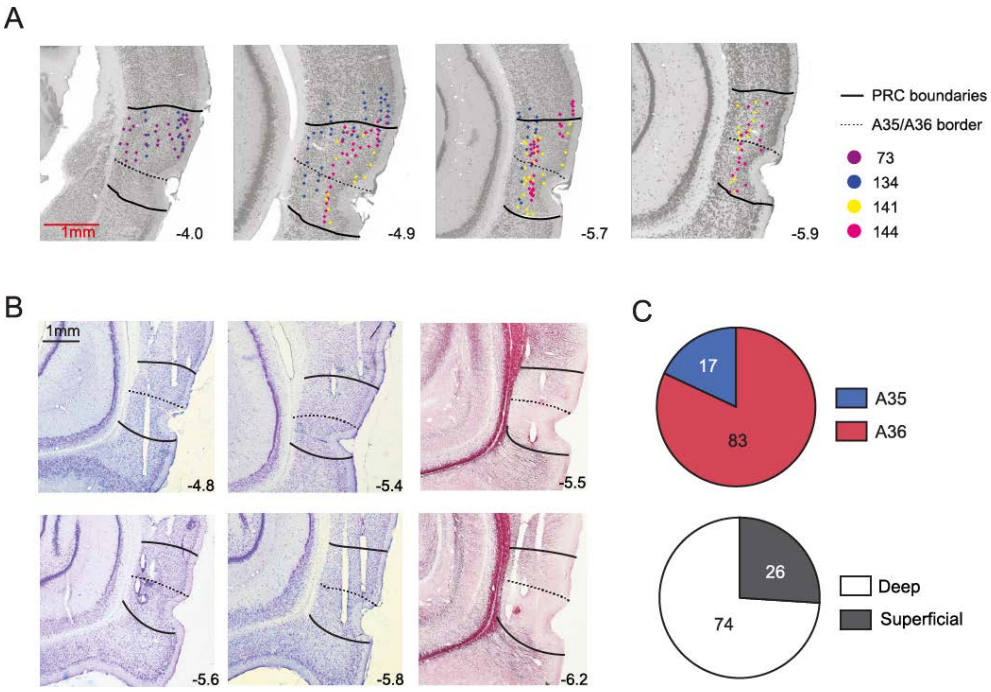

Figure 5. Histological verification of tetrode positions and the number of neurons recorded from the PER (**A**) The histological sections containing the PER were obtained from an online atlas (http://www.rbwb.org).Using those online images as templates, the locations of individual tetrodes were marked with dots (color-coded for different animals). Regional boundaries of the PER (solid lines) and its subfields A36 and A35 (dotted lines) were demarcated based on the online atlas and the standard atlas (Paxinos and Watson, 2007). Numbers indicate the relative positions of the sections from bregma. (**B**) Representative histological sections with tetrode tracks. The first and second columns show Nissl-stained tissues, and the third column shows myelin-stained sections. (**C**) Pie charts for showing the number of units in different subregions in the PER. Only units that satisfied the unit-isolation criteria and were used in the final analyses (upper, A35 and A36; lower, deep and superficial layers) are shown.

Table 1. The number of PER cortical neurons recorded across days (D)

Rat #	Region	Layer	D1	D2	D3	D4	D5	Sum
rat73	A35	deep	-	-	0 (1)	-	-	-
		superficial	-	-	-	-	-	-
	A36	deep	3 (30)	1 (20)	8 (38)	3 (28)	-	15
		superficial	0 (22)	2 (13)	3 (20)	2 (14)	-	7
rat134	A35	deep	-	-	0 (1)	-	-	-
		superficial	0 (1)	-	-	-	-	-
	A36	deep	7 (20)	6 (20)	2 (13)	7 (14)	-	22
		superficial	1 (8)	0 (9)	0 (9)	1 (8)	-	2
rat141	A35	deep	4 (8)	3 (7)	0 (6)	3 (3)	-	10
		superficial	-	-	2 (3)	1 (2)	-	3
	A36	deep	2 (2)	-	2 (2)	2 (2)	-	6
		superficial	0 (4)	1 (4)	0 (1)	-	-	1
rat144	A35	deep	-	-	-	-	-	-
		superficial	-	2 (3)	1 (5)	0 (1)	1 (1)	4
	A36	deep	7 (11)	1 (3)	5 (9)	5 (11)	3 (5)	21
		superficial	2 (5)	1 (5)	2 (9)	3 (9)	1 (5)	9

Cells that met the unit-quality criteria were only included. The total number of cells were indicated in parenthesis.

For the purpose of categorizing putative interneurons and pyramidal neurons, I plotted the spike width (measured between the peak and the trough in the average waveform) against its average firing rate (**Figure 6A**). Based on the scatterplot, the cells showing < 250 μs (n = 6) in spike width were categorized as putative interneurons, and the remaining neurons were categorized as putative pyramidal neurons (n = 94)(**Figure 6A**). Therefore, the majority of neurons used for analyses in the current study were putative pyramidal neurons. The mean spike width of interneurons was 171.88 ± 6.99 μs, and that of the pyramidal neurons was 430.52 ± 8.28 μs (mean ± SEM). The mean firing rates of putative interneurons and pyramidal cells were 1.77 ± 0.30 Hz and 3.64 ± 0.23 Hz (mean ± SEM), respectively. It is notable that all putative interneurons exhibited mean firing rates of < 3 Hz, and the results (the absence of high-firing interneurons) are in agreement with the previous report (Deshmukh et al., 2012).

I also examined the firing patterns of the putative interneurons and pyramidal neurons by drawing a spiking autocorrelogram for each unit (**Figure 6B**). Based on the autocorrelograms, I grouped the cells into the following three categories (Bartho et al., 2004): *(i)* bursting neuron, *(ii)* regular spiking neuron, and *(iii)* unclassified neuron. Specifically, the bursting neuron was characterized by a sharp and large peak at 3-6 ms with an exponential decay afterwards (**Figure 6B**, upper). Regular spiking neurons exhibited an exponential rise from 0 to tens of milliseconds, and the maximum bin value was detected at > 35 ms in the autocorrelogram (**Figure 6B**, middle). Cells that did not meet any of these criteria were labeled as “unclassified.” (**Figure 6B**, lower). Of the PER units recorded in the current study, 72 % were regular spiking neurons and 20 % were bursting neurons. The remaining 8 % were unclassified neurons (**Figure 6C**). I performed the same classification on the units excluded from the main analyses, and found that the majority (n=9) of the units were regular spiking neurons (cell 1 to 3 in **Figure 6C**) and only one unit was categorized as an unclassified neuron (cell 4 in **Figure 6C**).

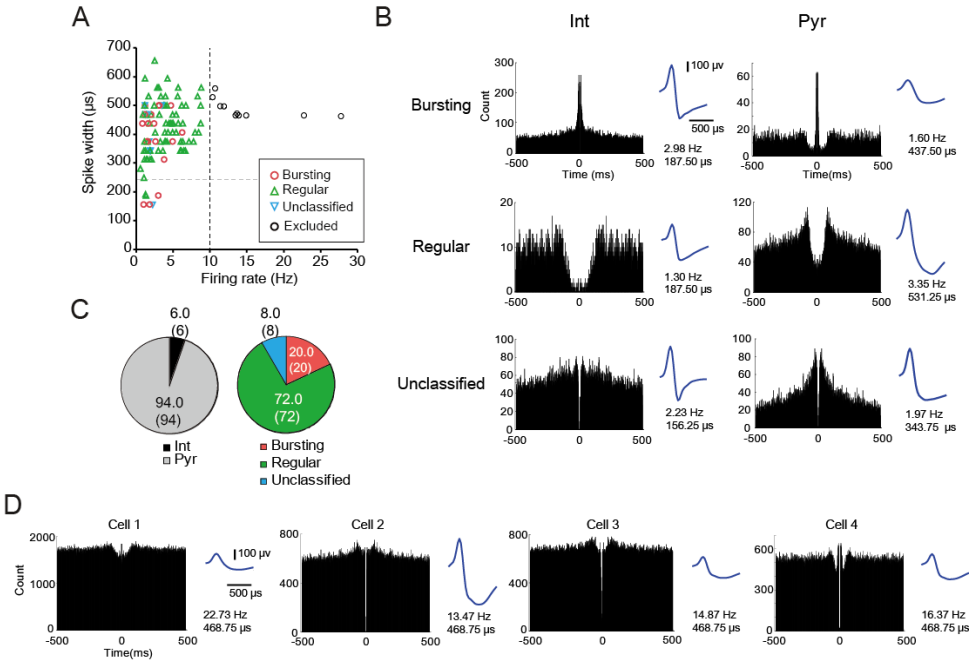

Figure 6. Classification of PER neurons (**A**) A scattergram showing the relationships between the average firing rate and the average spike width (peak-to-trough) of PER units recorded in the current study. The vertical dashed line indicates the firing criterion (10 Hz). Ten units were eliminated based on the criteria (black circles). The horizontal dashed line marks the cutoff point of a spike width (250 μs) that separated putative interneurons and pyramidal neurons. (**B**) Representative autocorrelograms (time window = ±500 ms, bin size = 1 ms) drawn for putative interneurons (Int, left) and pyramidal neurons (Pyr, right) in the PER. Shown on the right of each autocorrelogram is the averaged waveform of a neuron. The mean firing rate and spike width of a neuron were indicated below the waveform. On the basis of the autocorrelogram characteristics, cells were classified into bursting (upper), regular (middle), and unclassified (lower) categories. (**C**) Pie charts showing the percentage of putative interneurons and pyramidal neurons based on the spike width criterion (left), and the percentage of neurons categorized based on autocorrelograms (right). The number in the parenthesis denotes the number of units. (**D**) Representative autocorrelograms and waveforms of the 10 eliminated units based on the firing rate criteria.

Neural activity in the PER is strongly modulated by critical events in the OCSC task

I then examined whether neuronal firing in the PER was significantly modulated by the pre- and post-choice events, compared to the neuron's baseline firing rate (i.e., the average firing rate before the object onset). For this purpose, I constructed a peri-event rastergram with individual spiking times aligned in reference to the choice moment (**Figure 6**). The firing rates in the majority of single units (83%) were significantly changed from the baseline before and/or after the choice response was made. Specifically, some neurons (19%) changed spiking activity significantly only during the pre-choice period by increasing (cells 1 and 2 in **Figure 6A**) or decreasing (cells 3 and 4 in **Figure 6A**) their firing rates relative to their pre-object-onset baseline firing rates, and other units (22%) significantly increased or decreased their firing rates after the rat made a choice (post-choice period) (**Figure 6B**). The largest proportion of units (59%), however, significantly changed their firing rates from baseline for both pre- and post-choice periods (**Figure 6C**).

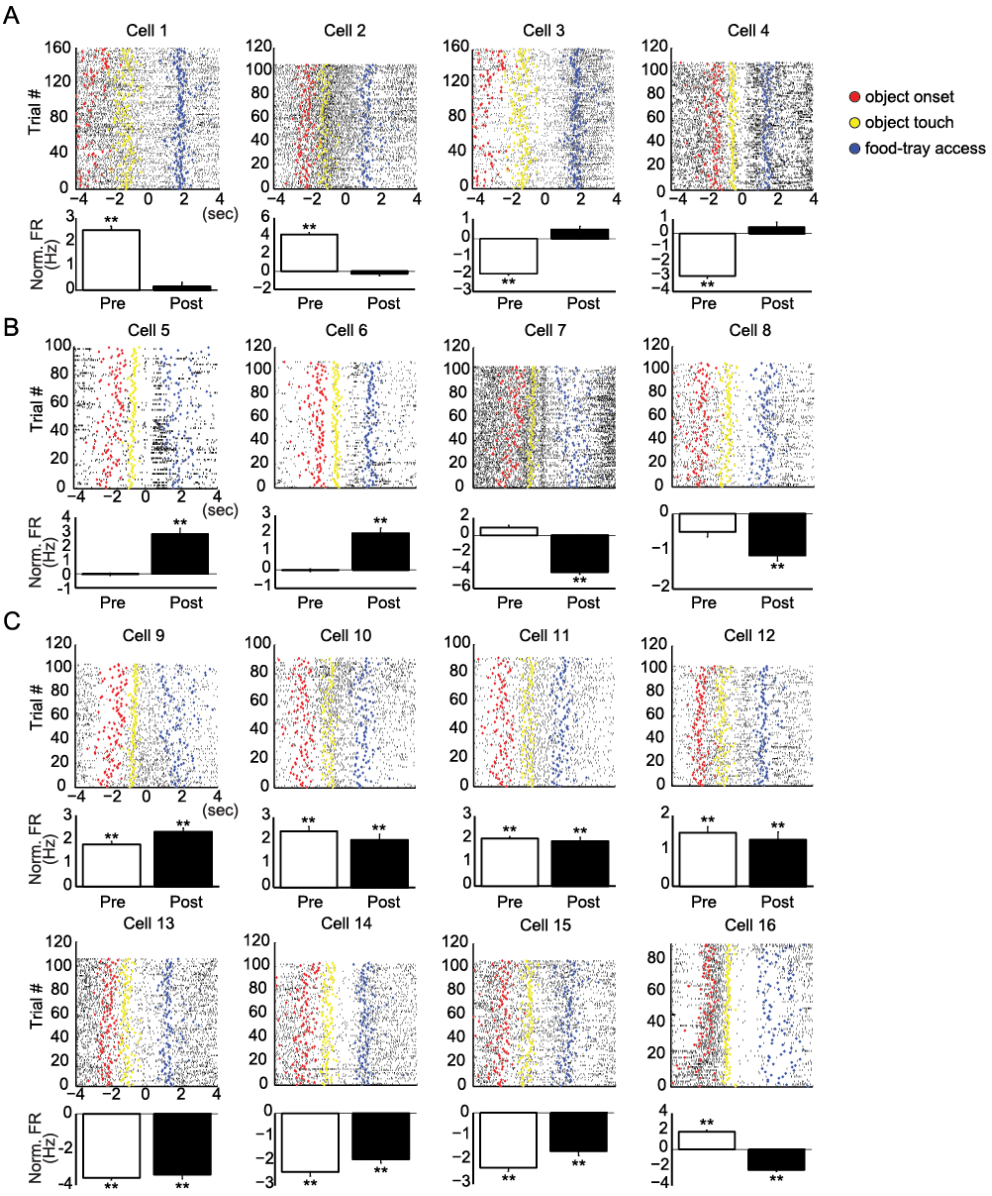

Figure 7. Choice event-related neuronal modulations in the PER (**A**–**C**) Raster plots (upper) and normalized mean firing rates (lower) of representative neurons in the PER showing the firing patterns in the pre- and post-choice periods. For each cell, individual spikes were aligned with the occurrence of the choice event. The colored dots in the raster represent the major events of the object-cued spatial choice task (red for object onset, yellow for object touch, and blue for food-tray access). Neuronal activity in the PER was significantly modulated relative to that of the

baseline (1s before the object onset) in the pre-choice period (**A**), post-choice period (**B**), or both (**C**). **$p < 0.01$. The firing rates associated with the event periods were normalized by subtracting the baseline firing rates.

With respect to the direction of the firing-rate change, neurons either increased or decreased their firing rates (compared with their baseline), and similar proportions of neurons showed opposite directional changes when the neurons were examined during the pre-choice period or during both the pre- and post-choice periods (F values < 2.00, p values > 0.16, chi-square test) (**Table 2**). However, those neurons demonstrating significant activity changes during the post-choice period were more likely to show excitatory patterns (72%) than inhibitory patterns (28%), relative to the baseline activity level (F = 7.11, p < 0.01, chi-square test). A few neurons (n=3) also exhibited mixed patterns, with increased discharge rates in one event period followed by decreased firing patterns in the other period (cell 16 in **Figure 6C**; **Table 2**).

Table 2. Firing patterns of event-responsive PER neurons

Event period	Response pattern (from baseline)		
	Excitation	Inhibition	Mixed
Pre-choice	6	10	-
Post-choice**	13	5	-
Pre- & Post-choice	26	20	3

(** $p < 0.01$)

Neuronal discharge in the PER is modulated by both the object cue and its associated response but not by the object alone

After establishing that, as described above, the majority of PER neurons (n = 83/100) were strongly modulated in association with the choice responses made during the task, I examined whether those units discharged disproportionately in association with critical task demands, such as object identity and spatial choice response. A two-way ANOVA was conducted for each neuron using the object category (Toy and Egg) and spatial choice (left and right) as factors. However, because these two factors were highly correlated in our study (especially in correct trials), this analysis alone might cause a multicollinearity problem. Therefore, a more conservative approach was adopted in which the ANOVA analyses were examined further by using additional t-tests (see **Materials and methods** for details).

To illustrate the relative magnitude of the neuronal responses associated with different trial conditions, I organized the data for each neuron into a bubble chart (**Figure 8A**), with the size of each circle indicating the relative response strength of a neuron for a particular object-choice paired association. For example, before the rat made its choice response (pre-choice), cell 1 in **Figure 8A** discharged more for left choices than for right choices, regardless of the cueing object. However, this neuron responded significantly to the interaction between the object and choice factors in the post-choice period because the cell showed higher firing rates relative to the other conditions when the rat touched the disc located on the right side after sampling the Toy object, or when choosing the disc located on the left side after sampling the Egg object. Notably, I rarely found a neuron in the PER that specifically responded only to a particular object during the pre-choice period regardless of spatial choices made (**Figure 8B**). Instead, in the pre-choice period, some neurons (27.7%, **Figure 8B**) fired specifically for a particular choice response, as illustrated by cell 1 and cell 2 for left and right choices, respectively (**Figure 8B**). Other neurons (6%) fired selectively for the interaction between the object and spatial responses. Similarly, in the post-choice period, neurons fired for a particular choice response (18.1%, cell 3 in **Figure 8A**) and for the interaction between object and response factors (51.8%,

cells 1, 2 and 4–6 in **Figure 8A**). The firing rate of only one neuron was significantly modulated by the object factor alone in the post-choice period. Neurons appeared to respond to the choice response factor more in the pre-choice period than in the post-choice period, although no statistical significance was found (F values < 3.60, p values > 0.06, chi-square test). By contrast, significantly more neurons responded to the interaction between the two factors in the post-choice period than in the pre-choice period ($F = 42.32$, $p < 0.0001$, chi-square test).

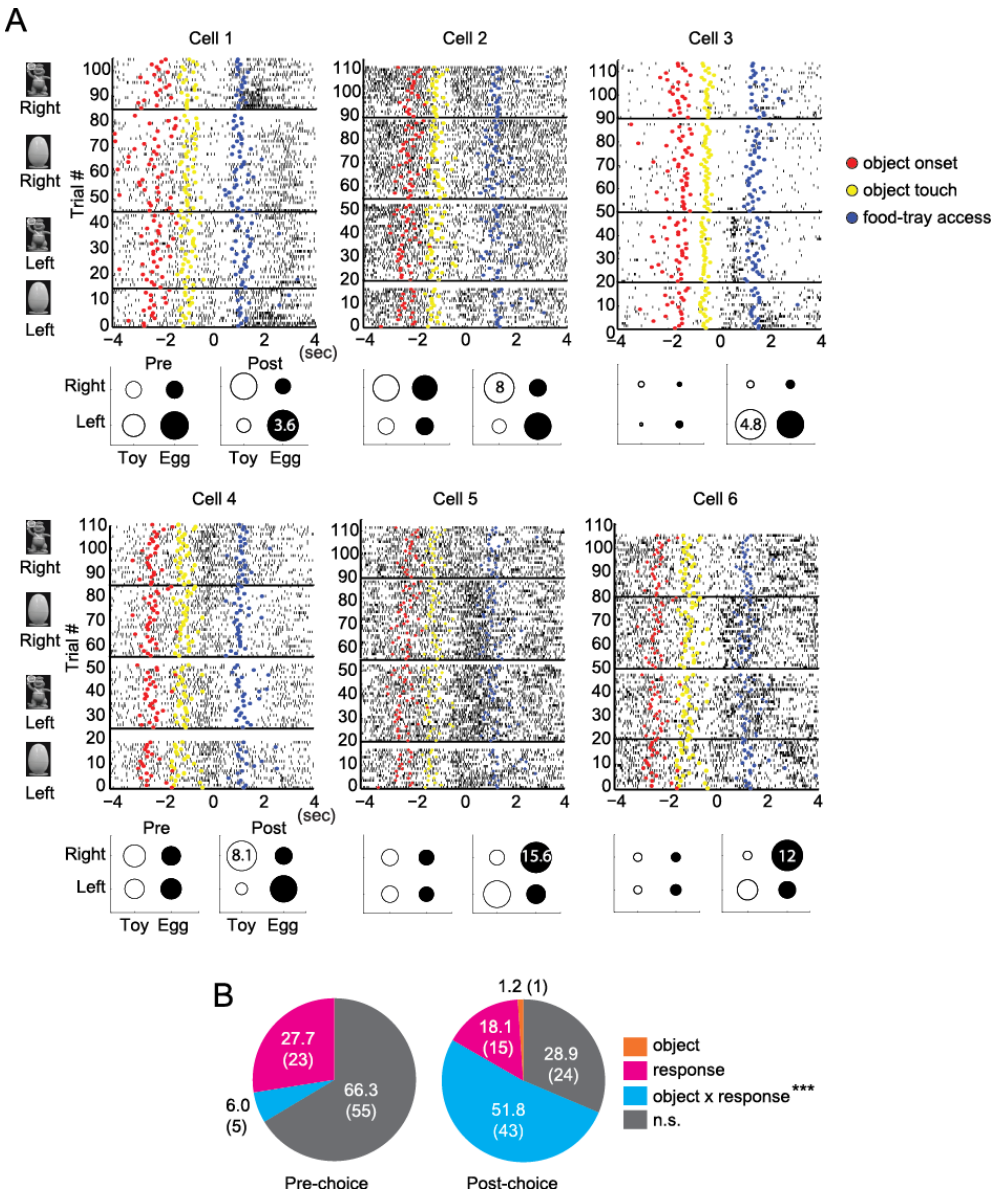

Figure 8. PER cortical neurons represent choice response and the object-choice contingency

(**A**) The raster plots were sorted according to four different object-choice contingencies (denoted by the object images and the responses on the left side of the raster plot). The bubble chart below the raster plot illustrates the relative response strengths of a neuron for different trial conditions. The number in a circle indicates the mean firing rate of the trial condition in which the maximal cell firing of the neuron was observed. The sizes of the other circles are scaled in proportion to the

maximal discharge rate. (**B**) Pie charts showing the percentage of neurons in the PER that respond significantly to the major task-related factors, such as object and spatial response factors, in the pre- and post-choice event periods. The numbers in the parentheses indicate the number of cells. Note that the proportion of PER neurons with a significant interaction effect between object and choice response factors significantly increased in the post-choice period compared to the pre-choice period. ***$p < 0.0001$.

Neuronal activity in the PER is influenced by perceptual ambiguity of object at the population level

I further investigated whether the level of ambiguity associated with the sample object modulated the activity levels of the individual response-selective PER neurons during the pre-choice period by running a two-way ANOVA (alpha = 0.05) with the ambiguity level and the choice response as main factors. Only a small fraction of neurons (n = 3) showed firing patterns significantly correlated with ambiguity, and no neuron showed a significant interaction between the response and the ambiguity level.

I subsequently examined whether the effect of ambiguity could be observed at the population level by constructing population rastergram associated with each object for the pre-choice period (**Figure 9A**, see **Materials and methods**). I noted that the similarity in population firing patterns associated with the original STD object became disrupted as the ambiguity level increased for both object categories (**Figure 9A**). The similarity between the population rastergrams was measured by calculating a Pearson's correlation coefficient between the STD object (ambiguity level 0) and its associated four AMB objects (ambiguity levels 1 to 4) (**Figure 9B**). There were interesting differences between the two object categories in terms of the changing patterns of the neuronal population across the ambiguity levels. Specifically, the similarity in the population activity decreased gradually for the Toy object (**Figure 9B**, blue line), whereas the similarity decreased abruptly at the ambiguity level 2 and remained at similar levels afterwards (**Figure 9B**, red line). The correlation coefficients for both object categories then converged to a similar level when the ambiguity levels were maximal.

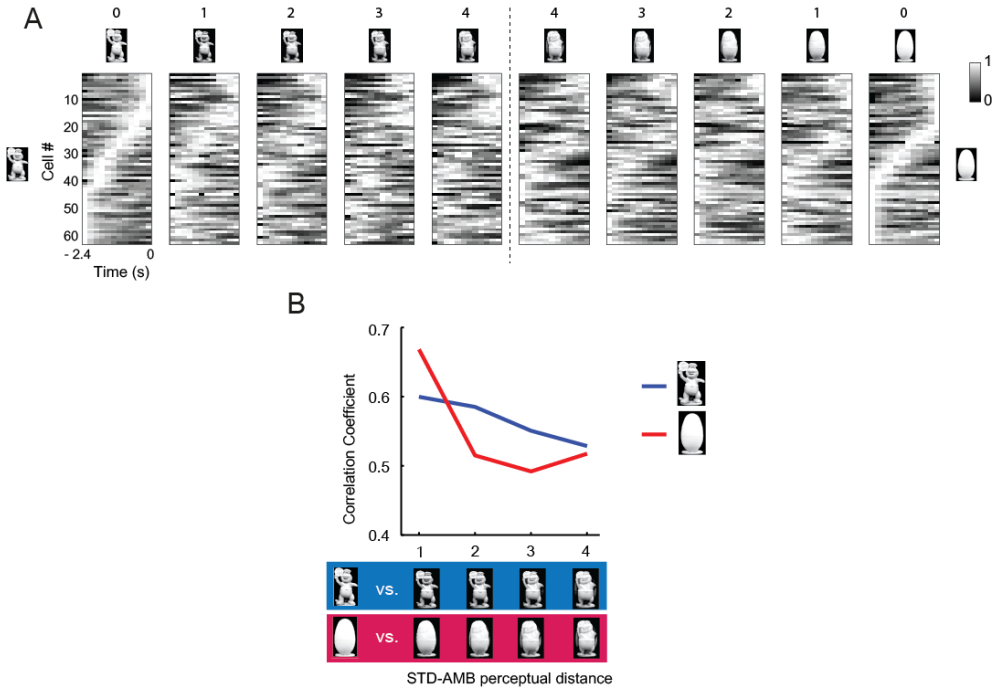

Figure 9. Effects of perceptual ambiguity on the response of the PER neuronal population in the pre-choice period (**A**) The population rastergram was constructed from all active PER neurons before the choice event for each object condition (time bin= 200 ms). The temporal bin associated with the highest firing rate was represented by using the lightest color. The cells were ordered according to the maximal firing location in the standard object condition for each object category. The number above each stimulus denotes the level of ambiguity. The vertical dotted line denotes the border between the two object categories. Note that the temporal firing patterns in the neuronal population were disrupted as ambiguity increased in both object categories. (**B**) Pearson's correlation coefficients were calculated between the population rastergram associated with the STD object and each of the four rastergrams associated with its morphed AMB objects (levels 1 to 4) in each category.

Neuronal firing in the PER is strongly modulated by choice outcome

As shown above (**Figure 8**), many PER neurons conveyed conjunctive information for the object identity and response, particularly in the post-choice period. I hypothesized that the significant neuronal modulations observed in the post-choice period might be closely related to the outcome of the choice response because auditory feedback was given immediately after a choice was made in the current task. However, because the auditory feedback might signal not only the outcome of a choice but also the presence or absence of a reward in the food tray at the same time, I examined whether the post-choice activity in the PER reflected the choice outcome or the expectation of a reward.

To dissociate the above possibilities, I first selected neurons that exhibited maximal firing rates in the post-choice period (n = 25). The peak firing locations in time in the post-choice period were different among PER neurons, with some units firing maximally immediately after the choice response (e.g., cell 1 in **Figure 10A**) and other cells showing longer peak latencies from the choice moments (cells 2–4 in **Figure 10A**). Overall, I found that the peak firing was more closely coupled to the moment of choice response than to the food-tray entry event in the post-choice period (median latency from choice-to-peak firing = 606 ms; median latency from peak firing to food tray entry = 882 ms; $Z = -3.00$, $p < 0.01$ in Wilcoxon signed-rank test) (**Figure 10B**). It is unlikely that these choice-related firing correlates reflected pure perception of the auditory feedback because prior studies showed that approximately 30–40 ms are required for an auditory signal to reach the PER (Furtak et al., 2007a). The above analysis was performed on correct trials only; however, the peak-firing locations for error trials were similarly coupled to the choice. The latencies from choice to peak firing rates measured after correct choices were not significantly different from those measured after error responses ($Z = -1.44$, $p = 0.15$, Mann-Whitney *U* test) (**Figure 10C**). These results indicate that the analyses using the peak-firing locations during the post-choice period were not significantly influenced by behavioral differences associated with correct and error responses. Overall, the results suggest that the significant neural activity observed in the post-choice period in the PER is closely related to the choice response itself and to its

outcome.

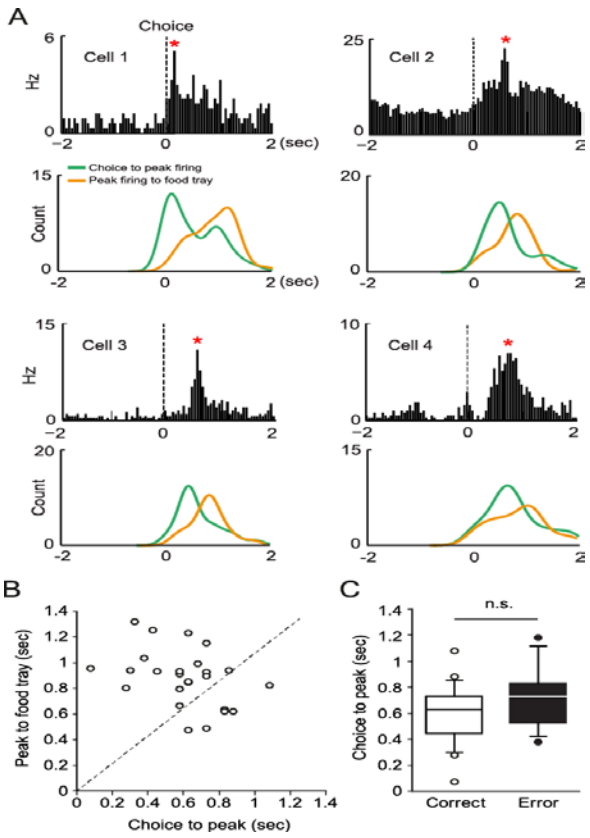

Figure 10. Activity of PER neurons in the post-choice period conveys trial outcome-related signals (**A**) The firing-rate distribution of a neuron in the PER is shown (top) 2 s before and after the choice responses (dotted line). The asterisk denotes the time bin in which the maximal firing rate was observed. Shown below is the histogram of the latency from the choice response to the peak-firing rate (green) and of the latency from peak firing to the food-tray entry (orange). Four representative neurons were chosen to show that the post-choice firing peaks were more closely related to the choice responses than to the food-tray entries. (**B**) The distribution of the medians of the temporal locations of the firing peaks with reference to the time points associated with the two events (choice response to peak firing and peak firing to food-tray access), illustrated in a scatter plot. Note that the PER units fired maximally closer to the choice event (x-axis) than to the food-tray entry event (y-axis). The dotted diagonal line denotes the points where the peak-firing location maintains equal distances from the two events. (**C**) Similar choice-to-peak latencies were observed in cells showing a peak firing following a correct response and those following an error.

Pre-choice neuronal activity in the PER better predicts the upcoming choice when followed by an error-driven feedback signal in preceding trial

The significant neural activity observed after the choice response (**Figure 10**) may function as a feedback signal for the outcome of that choice, which may, in turn, influence the animal's choice response in the next trial. Similar feedback signals have been reported in other brain areas, including the prefrontal cortex (PFC), striatum, hippocampus, and orbitofrontal cortex (Kepecs et al., 2008; Narayanan and Laubach, 2008; Histed et al., 2009; Wirth et al., 2009; Narayanan et al., 2013), but, to our knowledge, not in the PER. To test whether cells in the PER also exhibit similar properties, I categorized the post-choice outcome-selective neurons (n=43) into two subtypes based on their activity profiles: correct-up cells and error-up cells (Wirth et al., 2009). The correct-up cells increased their firing rates following correct choices (n=21) and the error-up cells did so following error responses (n=22) (**Figure 11A**). There was no proportional difference between two categories ($F = 0.05$, $p = 0.83$, chi-square test).

By using the ROC methods (see **Materials and methods**), I then investigated whether the neuronal activity in the pre-choice period in a given trial was a better predictor of the upcoming choice response when such activity was followed by significant neural activity in the post-choice period of the preceding trial. When ROC curves were plotted for correct-up cells and error-up cells, I noted that the cells in the error-up category seemingly predicted the upcoming choice response better (i.e., larger AUC) when an error-related feedback signal was present in the post-choice period in the preceding trial (PreT error in **Figure 11B**) compared with when a correct choice-related feedback signal was present (PreT correct). The cells in the correct-up category did not show such properties (**Figure 11C**).

To further quantify the above observations, I estimated the capability of predicting the choice response in the upcoming trial given the neuronal activity in the pre-choice period by calculating RPI (**Materials and methods**). In correct-up cells, the RPIs between the two trial types (i.e., trials following correct and error responses, denoted by PreT correct and PreT error, respectively, in **Figure 11C**) were not significantly different

from one another ($Z = -0.88$, $p = 0.37$, Wilcoxon signed-rank test), suggesting that the neural feedback in the post-choice period after correct choices (in correct-up cells) did not significantly influence the choice response in the next trial. The significant enhancement in the predictability of the upcoming response in the error-up neurons was observed only when the error was made in the immediately preceding trial (i.e., trial lag 1); that is, when the trial lag was increased to two or three, the RPI was not significantly different regardless of the outcome of those trials ($Z > -1.06$, p values > 0.28, Wilcoxon signed-rank test).

However, in the error-up neurons, the RPI was significantly higher for trials when the previous choices resulted in errors compared with trials having preceding trials associated with correct responses ($Z = -2.17$, $p < 0.05$, Wilcoxon signed-rank test) (**Figure 11C**). Higher RPIs in the PreT-error trials for the error-up neurons were observed in the majority of animals (3 out of 4 rats). The RPIs for the trials following the error-related feedback signals were also significantly higher than the baseline RPI obtained from 1,000 randomly shuffled trials ($Z = -2.17$, $p < 0.05$) in the error-up neurons, whereas no significant difference was found in the trials that were not associated with the feedback signals when tested using the same procedures ($Z = -0.38$, $p = 0.70$, Wilcoxon signed-rank test) (**Figure 11C**). For the correct-up neurons, both the RPIs from PreT-correct and PreT-error trials were not significantly different from the shuffled baseline (Z values > -1.72, p values > 0.08, Wilcoxon signed-rank test) (**Figure 11C**). These results suggest that the neural activity in the PER in the pre-choice period is significantly influenced by the error-driven feedback signal from the immediately preceding trial.

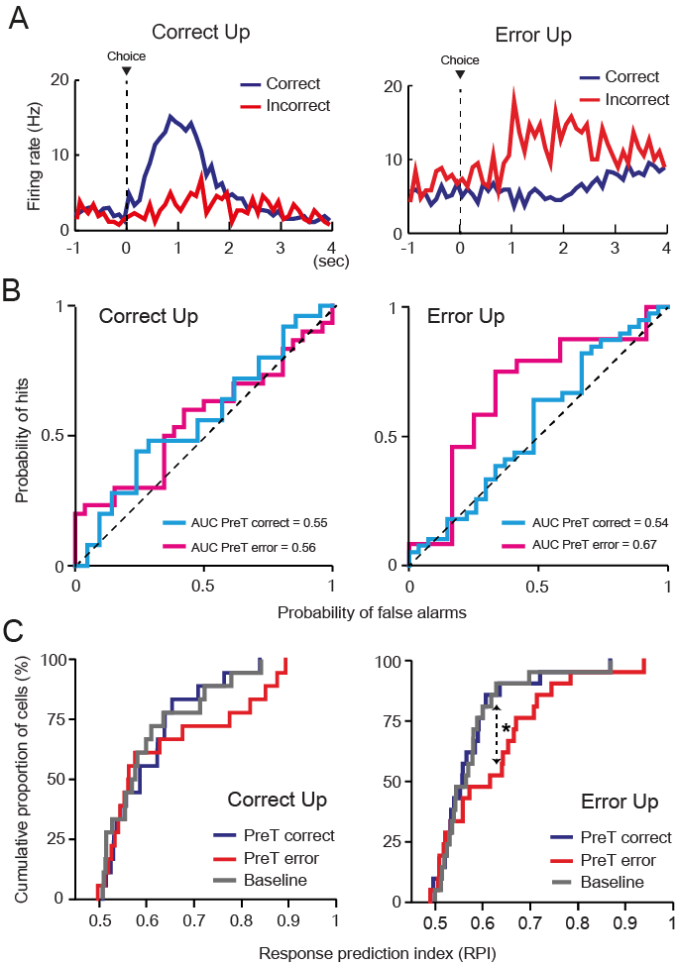

Figure 11. Error choice-related feedback signal in the post-choice period significantly affects the upcoming choice-related signals in the PER (**A**) Representative examples of the spike density plots of the correct-up cells (left) and error-up cells (right) in the PER. The correct-up cells exhibited an elevated firing response when correct choices were made compared to when errors were made, whereas the opposite was true for the error-up cells. (**B**) Representative ROC curves for the two types of outcome-selective neurons (correct-up and error-up cells). ROC curves were generated based on the firing-rate distributions associated with the choice responses (choices for the left and right discs). Each point of the ROC curve denotes the probability of neuronal spiking activity in a given trial being correctly assigned to one of the choice distributions ("hits") versus incorrectly assigned ("false alarms"). For the correct-up cells, the AUCs of the ROC curves were similar regardless of the presence of the neuronal feedback received from the previous trial. By

contrast, the AUC of the error-up cells was higher when feedback was received from the previous trial. (**C**) The response prediction index (RPI) was obtained for each outcome-selective neuron by averaging across the bootstrapped AUCs (1,000 iterations). In the correct-up cells, the RPI was similar regardless of whether the choice in the previous trial was correct (PreT-correct) or incorrect (PreT-error). In the error-up neurons, the RPI was higher in trials for which the previous choices resulted in errors (PreT-error). *$p < 0.05$.

Discussion

In the current study, rats discriminated the 2D object images successfully, and the inactivation of the PER impaired performance. PER neurons fired specifically for particular spatial responses, and more often, in conjunction with the cueing object, but the exclusive object-specific firing was rarely observed. The effect of perceptual ambiguity was minimal at the single cell level, but was visible at the population level. Many PER also neurons conveyed information about choice outcome, and I found that the error-driven post-choice neuronal feedback in a given trial increased the neuronal selectivity for the choice response during the pre-choice period in the following trial.

The PER has been viewed as an area critical for object recognition memory (Meunier et al., 1993; Ennaceur et al., 1996a; Buckley and Gaffan, 1998a; Winters and Bussey, 2005). However, PER neurons rarely signaled object-specific information before making a choice in our study, and the results appear incompatible with the primate literature (Brown et al., 1987; Miyashita and Chang, 1988; Liu and Richmond, 2000; Naya et al., 2003). Although most prior primate studies recorded neurons from a broadly defined inferotemporal (IT) cortex that includes the PER, TE, and entorhinal cortex, and thus more focused investigations on specific regions are needed in the future, some speculations can be made as to why an object-specific signal was not observed in the current study. First, it may simply be attributable to species-specific differences. Sensory and perceptual systems (especially the visual system) might be different between rodents and primates. For example, object recognition signals in the rodent brain may be identified at earlier processing stages (e.g., TE). It also needs considering that behavioral paradigms were very different between primate and rodent studies. Specifically, the above-mentioned primate studies employed a head-fixed design in which body movements were restricted and choices were made by a saccadic eye movement or a bar release (Miyashita and Chang, 1988; Miller et al., 1991; Liu and Richmond, 2000; Naya et al., 2001; Naya et al., 2003), whereas rodents are usually freely moving during testing.

Sensory dimensions associated with an object might also be critical in determining the involvement of the PER in object recognition memory. In most rodent studies, spontaneous object-recognition tasks were used in which rats were allowed to explore three-dimensional objects, presumably using multimodal sensory information (Burke et al., 2012; Deshmukh et al., 2012; Burke et al., 2014). A recent study reports a lack of repetition-induced response decrement in human visual association areas when three-dimensional objects were introduced as stimuli instead of two-dimensional images (Snow et al., 2011), and this may also be the case in animals. The rodent PER may be attuned to multimodal object information to integrate sensory inputs from multimodal systems (Burwell and Amaral, 1998; Kealy and Commins, 2011). These possibilities may need to be examined in future studies.

In the current study, the task required object information to be immediately translated into an appropriate spatial response for making a behavioral choice. Given such task demands, it should be critical for both nonspatial and spatial information to be conjunctively processed, possibly making communication between the PER and POR crucial. According to a theory of the spatial versus nonspatial information pathways in the medial temporal lobe, the PER is primarily concerned with nonspatial information, such as object information, whereas the POR is more involved in processing spatial information (Burwell, 2000; Hargreaves et al., 2005; Eichenbaum and Lipton, 2008; Henriksen et al., 2010). The results of the current study, as well as those of several previous studies, do not accord well with such a simplified view. For example, a recent study (Furtak et al., 2012) showed that single units in the POR conveyed conjunctive information for both object and place. Other studies also found that PER neurons exhibited location-specific responses in association with objects (Burke et al., 2012; Deshmukh et al., 2012).

Some of the recent theories position the PER at the final stage of visual perception in the ventral visual pathway (Bussey et al., 2005; Cowell et al., 2010), especially when individual features between objects overlap (Bussey et al., 2002; Lee et al., 2005; Murray et al., 2007; Baxter, 2009). The literature shows mixed results for the involvement of the rodent PER in ambiguous object recognition. Some studies reported

significant deficits (Eacott et al., 2001; Norman and Eacott, 2004; Bartko et al., 2007), whereas the opposite results were also reported (Clark et al., 2011). It is important to note that the supporting evidence for the perceptual roles of the PER was obtained mostly from behavioral studies using a concurrent object discrimination paradigm, and direct physiological evidence for the hypothesized role of PER has been lacking. In our study, the effect of object ambiguity was visible at the neuronal population level, but not at the individual neuronal level, and the results may provide a first physiological hint that the neuronal population in the PER may be involved in resolving ambiguity in object stimuli.

The ambiguity levels for two object categories affected the PER population responses differentially (**Figure 9**). That is, the PER neuronal population maintained STD object-related signal relatively better in the Toy object category than in the Egg object category. A close examination of the individual stimuli along the morphing continuum indicates that, for the Toy object, the morphing procedure influenced mostly the outer shape of the original stimulus, rendering more "Egg-like" shapes for the AMB objects, while the detailed within-object features were preserved across the morphing levels (**Figure 2B**). By contrast, for the Egg object category, the contours of the morphed Egg objects were largely preserved, but the within-object features associated with the Toy object became suddenly visible (against white background) even at the lower level of ambiguity (**Figure 2B**). The results suggest that detailed visual features of an object may provide more information to the PER than the shape and contour of the object.

There was a significant, outcome-dependent modulation of PER neuronal activity immediately after the rat made a choice response in our study. The increase in neuronal response might function as feedback for choice. Similar neurons have been documented in other brain regions, including the PFC, striatum (Histed et al., 2009), and hippocampus (Wirth et al., 2009) in primates, and the orbitofrontal cortex in rodents (Kepecs et al., 2008). In the Histed et al. study, for example, neurons in the PFC and the striatum increased direction-selective responses following correct trials in monkeys. Similarly, Wirth and colleagues demonstrated that primate hippocampal neurons with increased activity following correct trials (correct-up cells) displayed a stronger stimulus-

selective response that paralleled learning in an object-place associative task (Wirth et al., 2009). Similar observations were also made in the dorsomedial PFC in rats (Narayanan and Laubach, 2008), and the medial PFC in rats and humans (Narayanan et al., 2013) reported that the neuronal firing patterns in the dorsomedial PFC were significantly modulated following errors in a simple reaction-time task. Narayanan et al. (2013) also found that low-frequency oscillations within the area increased in both humans and rats specifically after error choices were made.

The results of our study bear some similarity with the results of the prior studies since the neural feedback signals in the PER were driven more by errors than by correct responses made during the preceding trials. Such error-driven signals may be attributable to the strong interconnections between the PER and the amygdala (Pitkanen et al., 2000; Kajiwara et al., 2003; Perugini et al., 2012). Reportedly, neurons in the amygdala increase activity in anticipation of an aversive outcome (Schoenbaum et al., 1998). Similarly, in humans, the amygdala is more engaged when declarative memory encoding is motivated by a threat of punishment than by an incentive (Murty et al., 2012). The interactions between the amygdala and the rhinal cortical regions are also facilitated when facing emotionally arousing stimuli, and the amygdala may provide a strong feedback to the PER once an error choice is made (Liu et al., 2000; Paz et al., 2006). Such negative feedback signal may strengthen the correct connections between objects and responses, and weaken incorrect object-response connections in the PER. The feedback-driven modulation following correct responses in our study might stem from dense dopaminergic projections to the PER from subcortical regions including the ventral tegmental area, ventral striatum, and substantia nigra (Schultz et al., 1993; Schultz, 1998; Li et al., 2003).

The results of the current study suggest that the roles of the PER may go beyond simply representing object memory in rodents, especially when a rat is required to make choices between different responses after recognizing an object. The PER may additionally represent a neural space in which a variety of object-associated variables (e.g., response requirements, emotional significance, and motivational feedback etc.) are represented dynamically in accordance with task demands.

Chapter 2. Neural correlates of the dual functions of the perirhinal cortex in both perception and memory for objects

Abstract

It has been controversial whether the perirhinal cortex (PER) is dedicated to either object memory or object perception. In the study, single units were recorded from the PER while the rat made paired associative spatial responses after sampling perceptually similar, continuously morphed objects. Examining the firing rates of cells as a function of the physical similarities among the morphed objects revealed two classes of neurons, namely, perceptual (P-cells) and mnemonic (M-cells) cells in the PER. The firing rates associated with the morphed objects changed monotonically in P-cells, matching the gradual changes in features of the morphed objects. However, the object-associated firing rates of M-cells exhibited stepwise changes at the choice border associated with different mnemonic responses, and the animal's performance was significantly predicted by the M-cell's activity. The findings suggest that the PER is involved not only in perceptually discriminating feature-ambiguous objects but also in recognizing the objects based on their mnemonic properties.

Keywords**:** object perception, object recognition, pattern separation, perirhinal cortex

Introduction

Animals, including humans, can recognize an object despite constant variations in its physical features (i.e., invariant object recognition). It has long been suggested that the perirhinal cortex (PER) plays critical roles in such object recognition memory (Meunier et al., 1993; Ennaceur et al., 1996a; Ennaceur and Aggleton, 1997; Winters and Bussey, 2005), mostly based on the results from behavioral paradigms in which an object must be recognized as a previously experienced object when it reappears against a novel one after a delay. In those tasks, damaging the PER produced significant delay-dependent performance deficits (Meunier et al., 1993; Ennaceur et al., 1996a; Ennaceur and Aggleton, 1997; Winters and Bussey, 2005).

While the traditional theories have investigated the roles of the PER within the mnemonic domain based on the delay-dependent memory impairment, a relatively recent line of research states that the PER is important not only for object recognition memory, but also for object perception when there is a significant amount of "feature ambiguity" between objects (Bussey et al., 2002; Lee et al., 2005; Bussey et al., 2006; Murray et al., 2007). In those studies, animals were trained to concurrently discriminate between different sets of objects sharing common features (e.g., AB+ vs. AC-, AB+ vs. BD-), and more severe deficits were found following PER lesions in high feature-ambiguity conditions, compared to low or intermediate ambiguity conditions (Bussey et al., 2002; Lee et al., 2005; Bussey et al., 2006; Murray et al., 2007). This perceptual-mnemonic theory posits that a conjunctive representation of an object is formed and stored in the PER as its individual sensory features are processed from lower to higher sensory cortical areas (Kravitz et al., 2013), and the resulting object representation in the PER resolves potential feature ambiguity.

The debate on the mnemonic *versus* perceptual roles of the PER in object information processing has been ongoing (Baxter, 2009; Suzuki, 2009; Suzuki and Baxter, 2009; McTighe et al., 2010; Clark et al., 2011), but remains unresolved largely because (i)

the key issues have been addressed mostly based on behavioral studies which yielded conflicting results so far across different laboratories, and, more important, (ii) there has been no physiological study that has directly addressed the issue with a proper experimental design. In the current study, I trained rats in a task that required both perceptual and mnemonic object information processing while recording single units in the PER. Specifically, rats learned to sample an object by touching an object image on a touchscreen monitor. Immediately after the object disappeared, a choice response associated with the sampled object should be made between two discs displayed on the monitor for rats to obtain reward. It is important to note that the task required the animal to pay attention to detailed visual features of a cueing object (requiring perception) and, at the same time, some perceptual information needed to be either ignored or taken into account for a discrete choice (requiring associative memory) to be made.

I have shown in the previous chapter that the PER is necessary in this task. Given the task demand, it is conceivable that perceptual processes are more required during the object-sampling period than in the choice period, and *vice versa* for mnemonic processes. By taking a different analytic approach that separated the pre-choice event period in the previous chapter further into object sampling period and choice period, I examined whether PER neurons exhibited differential firing patterns across those two event periods.

Materials and methods

Behavioral paradigm

The same behavioral and neural data obtained from the ambiguity sessions (AMB) in the first chapter were used, but different analytic approaches were taken. In chapter 1, the event period was defined as the pre-choice period (object onset to disc choices) and post-choice period (disc choice to foodtray access) (**Figure 2A**). For the present analyses, however, the pre-choice period was further divided into two event periods: (i) *object-sampling period* (from object onset to object touch) during which the object stimulus was visible on the screen and touched, and (ii) *choice period* (from object touch to choice) during which two discs appeared on both sides, and the rat was required to choose one of them in the absence of the cueing object (**Figure 12**). There was no delay imposed between the two event periods. The order of presenting the morphed objects across trials was pseudo-randomized, and the rat experienced all objects equally.

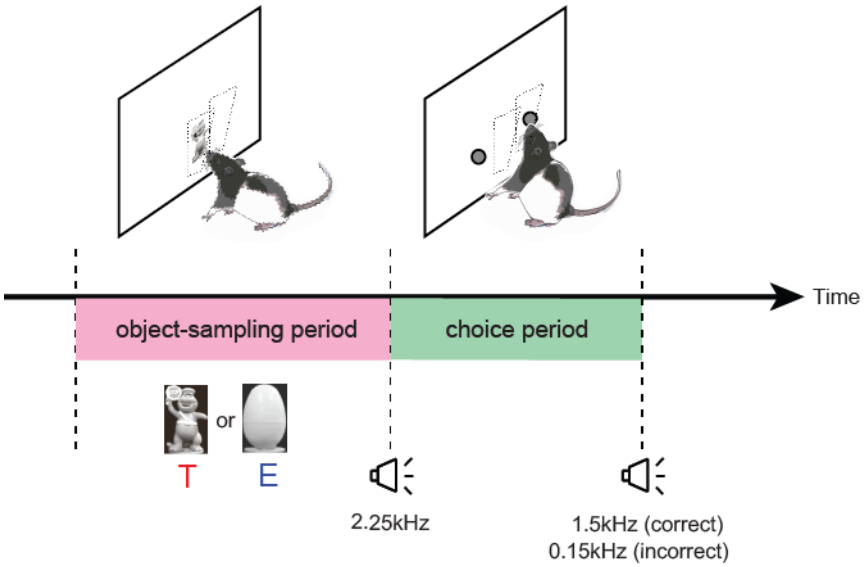

Figure 12. Event period definition. A cartoon of the rat performing the task with a schematic illustration of event epochs (object-sampling period and choice period) in the object recognition task. When the rat touched the object image on the touchscreen, the object cue disappeared with a 2.25 kHz tone and was immediately replaced by two response discs. The rat subsequently touched the object-associated disc and the trial terminated with an auditory feedback (1.5 kHz for correct and .15 kHz for incorrect choices). The object-sampling period (pink) was defined as from the object onset to object touch, and the choice period (green) from object touch to disc choice.

Data analysis

Unit-screening criteria

The following set of criteria was applied to screen neurons for analyses: (a) isolation distance ≥ 10 and an L-ratio ≤ 0.3, (b) average firing rate during at least one event period > .5 Hz, and (c) cells with the mean firing rate < 10 Hz in a session.

Physical object dissimilarity index

Physical similarity between object stimuli was quantified by calculating the pixel-by-pixel Euclidean distance between one standard image and other images across object images. The resulting values were mapped between 0 (e.g., the original Toy image being compared with itself) and 1 (e.g., the original Egg image being compared with the original Toy image).

Curve-fitting procedures for object-tuning curve

Discharge rates for 10 morphed objects were calculated from the correct trials for each event period and normalized from 0 to 1 for all PER units (> .5 Hz for either event period). The object category with the higher firing rates were positioned on the right-hand side, and the data were fitted with the following set of model equations.

(1) Quadratic model: $\alpha + \beta * \mathrm{obj} + \gamma * \mathrm{obj}^2$

(2) Four-parameter sigmoid model:

$$\gamma_{\min} + \frac{(\gamma_{\max} - \gamma_{\min})}{(1 + \ e^{(-\alpha * (\mathrm{obj} - \ \beta))})}$$

, where γ_{max} and γ_{min} denote upper and lower asymptotes, respectively, and α and β indicate a growth rate and inflection point, respectively. Obj denotes object stimuli. Bayesian information criteria (BIC) were applied to the two models, and the model yielding a lower BIC value was selected as the best-fit model for a given neuron. Only the neurons that

showed sufficient fitting to the model ($R^2 \geq .3$) were used for further analyses. The neurons fitted with the sigmoidal model were discarded if the inflection point fell outside the object range (from 1 to 10). The neurons that were best-fit with the quadratic model were named perceptual cells (P-cells), and those affiliated with the sigmoid model mnemonic (M-cells). Population tuning curves were obtained separately for the P-cells and M-cells by averaging across the individual tuning curves, and fitting the quadratic and sigmoid models to the data, respectively.

Linear classification

Linear discriminant analysis was performed to quantify how well a given neuron could predict the category of an object stimulus on the basis of firing rates. For each neuron, an N-dimensional vector composed of trial-by-trial firing rates was built, where N denoted the total number of trials. A firing rate from a trial was singled out as a test vector while all other trial vectors were used to train a linear classifier for assigning the test vector into one of the object categories. This “leave-one-out” cross-validation steps were repeated for every trial. Classification performance was measured by counting the proportion of correctly classified trials out of all trials per session.

Results

PER single units were recorded in the object memory task with ambiguous objects

Four male Long-Evans rats were trained in a touchscreen-based object memory task. Once the rat learned the task (≥70% correct responses for two consecutive sessions), a hyperdrive carrying 16 tetrodes was implanted for targeting the PER. During postsurgical testing, the two original images were digitally morphed into each other to create ten different, feature-ambiguous object stimuli (T5 to E5 in **Figure 13A**). Along the morphed object dimension, half of object stimuli (T1 to T5) closer to the original Toy figure were associated with the left disc and the other half (E1 to E5) were associated with the right disc, requiring rats to make discrete categorical choices in response to continuously changing stimuli (**Figure 13A**). The physical differences between the ambiguous stimuli (object dissimilarity index, see **Materials and methods**) increased in a curvilinear fashion along the morphing dimension (**Figure 13B**). Behaviorally, rats were affected by the physical ambiguity in object stimuli, showing a significant decrease in performance as a function of increasing feature ambiguity (**Figure 13C**; $F_{(4,64)}= 29.68$, $p< 0.0001$, repeated-measures ANOVA). Importantly, however, the performance of the rat was significantly higher than chance across all ambiguity levels (**Figure 13C**; t's> 4.41, p's< 0.0001 by Bonferroni-corrected t-test), suggesting that rats were able to discriminate among and generalize across the stimuli with high perceptual ambiguity.

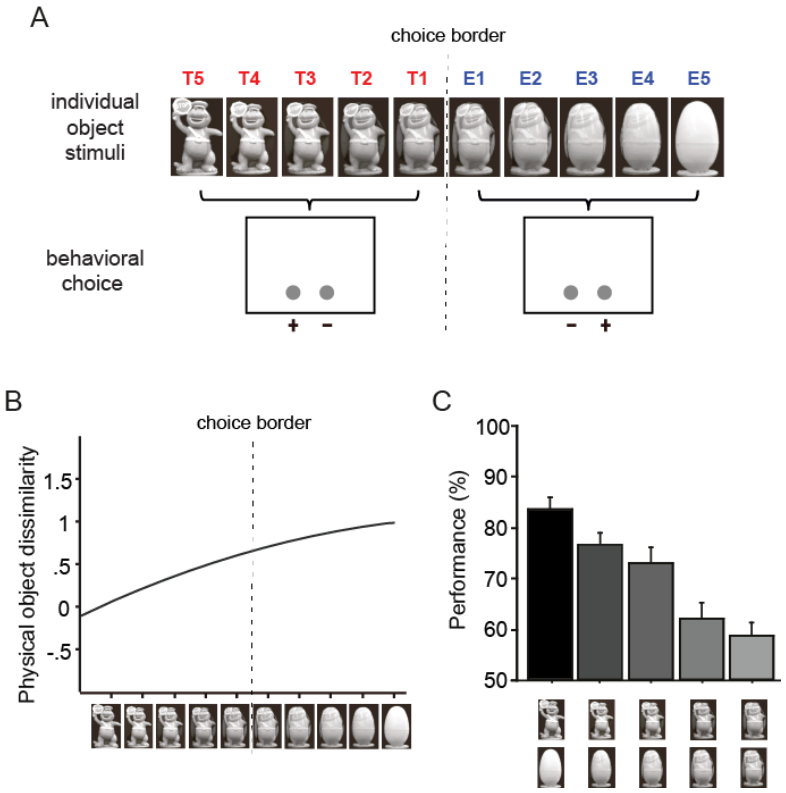

Figure 13. Feature-ambiguous object stimuli and behavioral performance. (**A**) The images of two original objects were morphed into each other to yield 10 object images differing in the amount of feature overlap. Each object was named by combining the object category (initialed as T for Toy and E for Egg) with the serial position (1 to 5) along the object-morphing spectrum. The choice border was set in the middle of the morphing continuum (between T1 and E1) and all objects in the same category required the same behavioral choices (denoted by '+' for reward and '-' for no reward for illustration purposes). (**B**) The level of physical object dissimilarity calculated between the original object and one of the morphed objects (including the original ones). (**C**) Behavioral performance as a function of increasing feature ambiguity.

I recorded spiking activities of single units in the PER while the rat performed the object memory task. Only the units that met the criteria (n = 128) were used in final analyses.

Perceptual and mnemonic firing patterns of neurons in the PER

To examine whether single units in the PER exhibited physiological correlates for perceptual processes (for representing individual features of objects) as well as for mnemonic responses, for each unit, the firing rates associated with individual objects were normalized from 0 to 1 in each event period (i.e., sampling period and choice period). The normalized firing rates associated with morphed objects were oriented in a scatter plot in such a way that the object category associated with higher firing rates ('preferred category', or P) was positioned on the right-hand side, and the 'non-preferred category' (NP) on the left-hand side (**Figure 14A**).

For each neuron that showed significant neural responses (> 0.5 Hz) during either event period, the tuning curve that best described the relationships between the morphed objects and the corresponding firing rates was determined by fitting either a quadratic or sigmoidal function to the data (**Materials and methods**). Then, I determined the best fitting function for each neuron by calculating Bayesian information criteria (BIC) for both sigmoidal and quadratic functions for each neuron's response profile. The fitting model associated with the smaller BIC value was chosen as the neuron's object-tuning curve. In the current study, I called a neuron 'perceptual cell' (or P-cell) if the neuronal response profile was best fitted by a quadratic model, and 'mnemonic cell' (or M-cell), if fitted best by a sigmoidal model (**Figure 14B**). Neurons showing relatively poor fitting ($R^2 < 0.3$) or the ones with the inflection points outside the object range (from 1 to 10) were excluded from analyses.

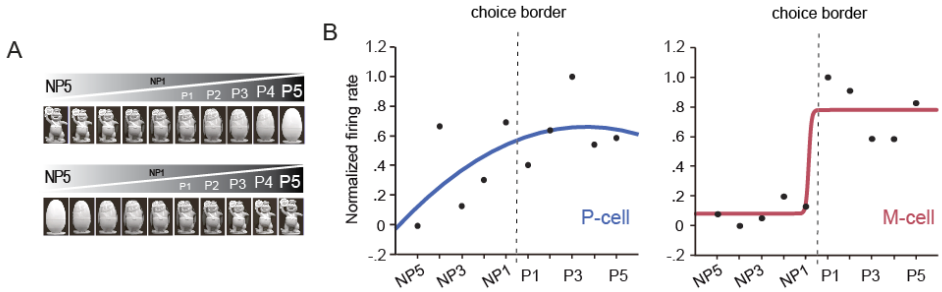

Figure 14. P-cell and M-cell in the PER. (**A**) For drawing an object-tuning curve, for each neuron, the object category associated with higher firing rates ('preferred category' or P) was positioned on the right-hand side, and the 'non-preferred category' (or NP) on the left-hand side. (**B**) Representative examples of curve fitting for P-cell (fit by a quadratic model) and M-cell (fit by a sigmoid model). Filled circles denote the normalized firing rates for each morphed object.

Interestingly, I found P-cells and M-cells in both event periods (**Figure 15**). The presence of a neuronal class in the event period that may not be compatible with task demands (i.e., M-cells in the sampling period and P-cells in the choice period) might reflect the nature of the representations in the PER. It could also be attributable to the fact that there was no delay in our task between the object-sampling and the choice period resulting in a potential gray transition period between two event periods. The proportion of P-cells (60%, n= 25/41; cells 1 to 5 in **Figure 15A**) was higher than the proportion of M-cells (39%, n= 16/41; cells 6 to 8 in **Figure 15A**) in the object-sampling period. During the choice period, this trend was reversed, resulting in a decrease in the proportion of P-cells (45%, n= 28/61; cells 9 to 11 in **Figure 15B**) and increase in the proportion of M-cells (54%, n= 33/61; cells 12 to 16 in **Figure 15B**) (**Figure 15C**).

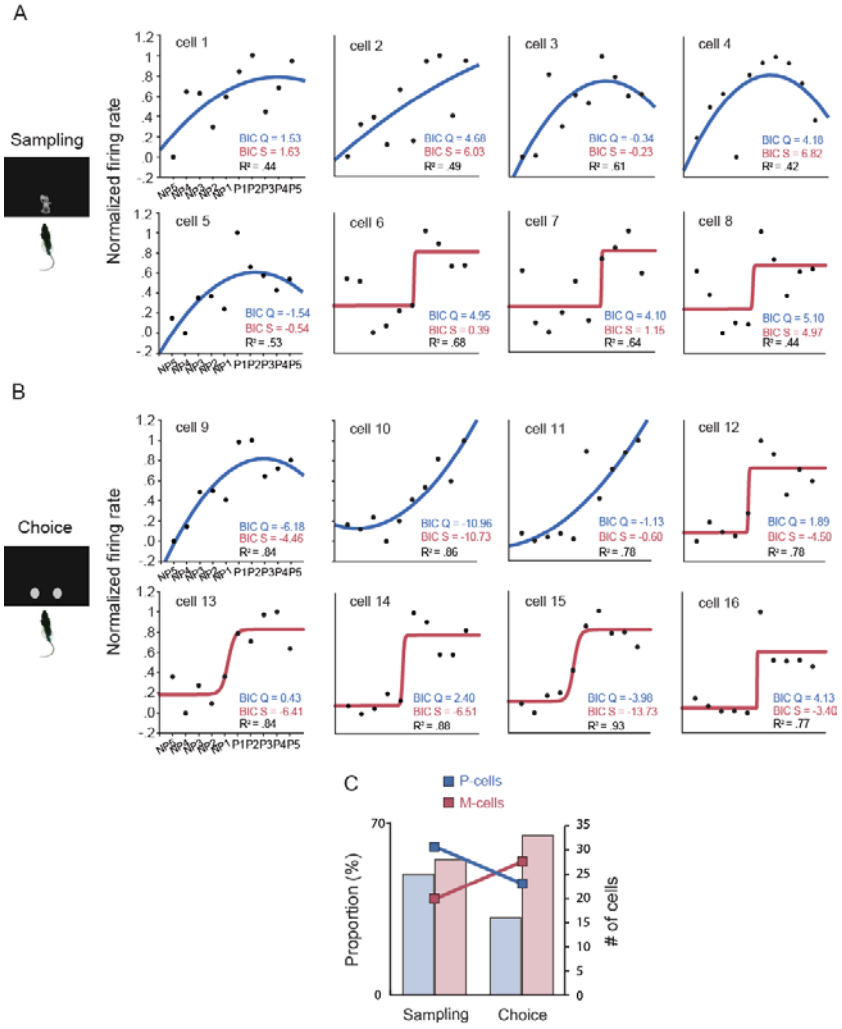

Figure 15. Distributions of P-cells and M-cells in the object-sampling period and the choice period. (**A**-**B**) Representative examples of object-tuning curves obtained from single units during the object-sampling period (**A**) and the choice period (**B**). Each neuron was fit with a quadratic (Q) or sigmoid (S) model and the optimal model was selected based on the BIC value. R2 measured the tightness of curve fitting. (**C**) The line graphs indicate the proportions of P-cells and M-cells in the sampling and choice period. The overlaid bar graphs denote the number of neurons *p < 0.05.

The object-turning curves for the above described neurons (87.5%, n= 70/80) were best fit with either a quadratic or sigmoidal model at least in one event period (**Figure 16A** to **Figure 16F**). Interestingly, some neurons (**Figure 16I**; 12.5%, n= 10/80) dynamically switched their response profiles across the event periods, showing a perceptual response during the sampling period and a mnemonic response during the choice period (**Figure 16G)**, or *vice versa* (**Figure 16H**). No layer-specific differences were found (F= 0.93, p = 0.66, Chi-square test) in the proportions of P-cells and M-cells [P-cells: 42% (n= 24/57) from deep layers and 52% (n= 12/23) from superficial layers]; M-cells: 44% (n= 25/57) from deep layers and 39% (n= 9/23) from superficial layers); P&M cells: 14% (n= 8/57) from the deep layers and 9% (n= 2/23) from superficial layers].

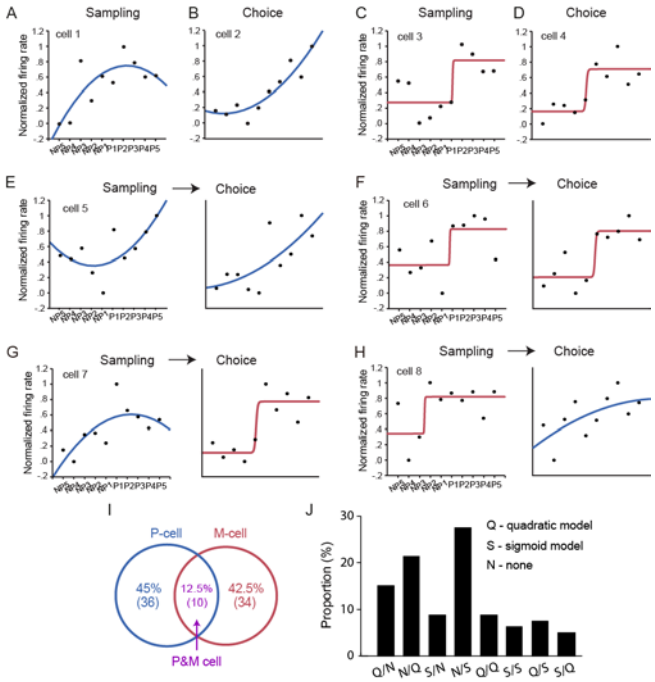

Figure 16. Distinct, but overlapping populations of P-cells and M-cells in the PER. (**A-D**). A representative example of neurons that showed perceptual (**A-B**) or mnemonic responses (**C-D**) during either sampling or choice period. (**E-F**). Representative neurons that yielded the same response profiles ((**E**) for perceptual and (**F**) for mnemonic responses) irrespective of the event type. (**G-H**). Representative neurons that exhibited dual response profiles, i.e., perceptual response during sampling and mnemonic response during choice (**G**), and *vice versa* (**H**). (**I**). A Venn diagram showing the proportions of P-cells and M-cells. The intersection of the two circles represents the neurons (P&M cells) fitted by both quadratic and sigmoidal functions across the event periods. The number in the parenthesis indicates the number of units. (**J**). The proportion of each neuronal type. "Q/N" indicates the neurons whose responses were best-fit to the quadratic model during the sampling period, but no fitting to either model during the choice period while "N/S" represents the neurons best-fit to the sigmoidal model only during the choice period.

Task demand-specific firing properties correlated with performance

To examine whether the firing properties of P-cells and M-cells were correlated with the animal's performance in the task, I obtained the object-tuning curves separately for correct and error trials. When the firing rates from the incorrect trials were fitted with the same model chosen as best for correct trials for the cell, the tuning properties were markedly disrupted. Specifically, data points were not as tightly fit to the tuning curve as in correct trials when the rat made errors in both the object-sampling (**Figure 17A**) and choice periods (**Figure 17B**). Furthermore, the tuning curves of M-cells became noticeably flattened near the choice border (e.g., cell 3 in **Figure 17A**; cells 7, 8, 9, and 12 in **Figure 17B**) and/or were off-tuned such that the inflection point was found off of the choice border (e.g., cell 4 in **Figure 17A**; cells 10 and 11 in **Figure 17B**).

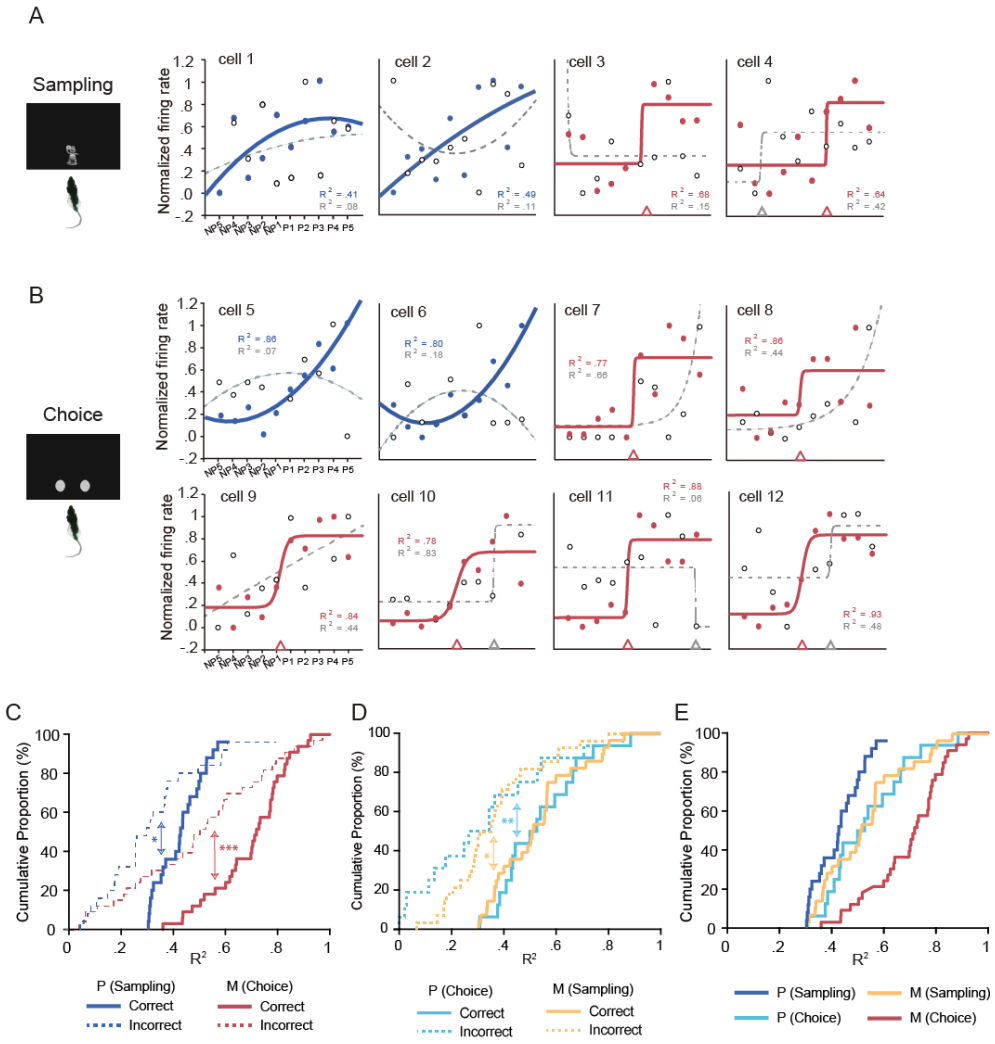

Figure 17. Comparison of object-tuning curves between correct and error trials. (**A-B**) Normalized firing rates from error trials (open circles) were fit with the same fitting model obtained from the correct trials (filled circles). The two curves obtained from correct (solid curves) and error trials (dashed curves) were overlaid to illustrate how the tuning characteristics were affected by task performance. For M-cells [cells 3-4 in (**A**) and cells 7-12 in (**B**)], the inflection points of the curves were indicated by arrowheads on the abscissa. The inflection points from the incorrect trials were marked with gray arrowheads on the same axis (omitted if the inflection point fell out of the object range). (**C**) Cumulative proportions of R^2 values that quantify the goodness-of-fit of the tuning curves of P-cells and M-cells. The neurons showing optimal responses (P-cells (P, blue) and

M-cells (M, red) from the sampling and choice period, respectively) were drawn together with those obtained from the error trials (dashed line). (**D**) The cumulative histograms of R^2 values from neurons showing non-optimal responses for task demand (i.e., P-cells (cyan) from the choice period and M-cells (yellow) from the sampling period). The histograms from error trials were overlaid in dash. (**E**) Cumulative proportions of R^2 values from neurons showing non-optimal responses for task demand (i.e., P-cells from the choice period and M-cells from the sampling period) were drawn together with those showing optimal responses. *$p < 0.05$, **$p < 0.01$, ***$p < 0.001$.

I ran quantitative comparisons on the goodness-of-fit (R^2) and the inflection points of tuning curves that were considered to be optimized for task demands (i.e., P-cells from the sampling and M-cells from the choice period). During the object-sampling period, the goodness-of-fit (measured by R^2) of P-cells decreased significantly in error trials, compared to correct trials ($Z= -2.54$, $p < 0.05$; **Figure 17C**). This was also the case for the M-cells during the choice period, which exhibited a significant difference between the correct and incorrect trials ($Z= -3.45$, $p < 0.001$, signed-rank test; **Figure 17C**). The goodness-of-fit of neurons with the response patterns that might not be optimal for task demands (i.e., P-cells during the choice period, or M-cells from the object-sampling period) also decreased in error trials relative to correct trials ($Z's< -2.53$, $p's < 0.05$; **Figure 17D**). However, the R^2 values of these non-optimal neurons were intermediate to those of the P-cells from the sampling period and the M-cells from the choice period (**Figure 17E**). Importantly, during the choice period, the R^2 values of M-cells associated with the correct trials from the choice period were by far the greatest, compared to other conditions ($p< 0.01$, Kolmogorov-Smirnov test).

The tuning characteristics of the M-cells were further examined by plotting the R^2 values against the inflection points (**Figure 18**). In correct trials, the M-cells showed a tight fit (mean $R^2 = 0.64$), with their inflection points clustered near the choice border (mean= 5.53, s.d.= 1.75). By contrast, the same neurons exhibited loose fit (mean $R^2= 0.44$) and relatively scattered inflection points (mean= 4.14, s.d.= 2.41) in error trials (**Figure 18**). These results strongly indicate that individual visual features of objects and their associated mnemonic responses were more reliably represented at the single neuronal level when the rat made correct choices than when making errors in the PER.

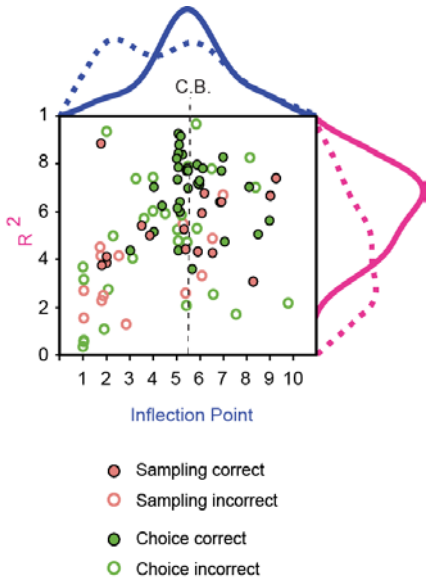

Figure 18. The relationships between the inflection points (abscissa) and goodness-of-fit (R^2, ordinate) of M-cells from the two event periods. Solid and dashed lines denote correct and incorrect trials, respectively. C.B. stands for the choice border. Note that the inflection points from the correct trials are centered at around the choice border (from 5 to 6) whereas those the error trials became more dispersed. The distribution R^2 values from correct trials were negatively skewed, but became more positively skewed in the error trials.

Monotonic perceptual discrimination *versus* mnemonic orthogonalization of ambiguous objects by the population of neurons in the PER

I subsequently examined whether the dual (i.e., perceptual-mnemonic) coding properties observed at the single-unit level were also observed at the neural population level in the PER. For this purpose, the individual object-tuning curves associated with the two neuronal classes, i.e., perceptual and mnemonic classes, were averaged for each class, and fitted with the quadratic model for the perceptual class and with the sigmoid model for the mnemonic class.

During the object-sampling period, I replicated the proportional results previously observed in individual neurons at the population level by showing that the population object-tuning curve for P-cells increased monotonically in a curvilinear fashion across the morphed objects, as if to reflect the increasing physical dissimilarity of the objects (Pearson's R between the two curves = 0.97; **Figure 19A**). More important, in the choice period, the population tuning curve for M-cells increased in a stepwise fashion, exhibiting a sharp nonlinear transition from one state to the other across the choice border (**Figure 19A**). By contrast, the population object-tuning curve of P-cells in the choice period did not follow the physical object dissimilarity curve as closely as in the object-sampling period (Pearson's R= 0.93, **Figure 19B**), exhibiting a larger growth rate during the presentation of the preferred objects. Furthermore, the mnemonic population tuning curve during the sampling period exhibited a relatively linear transition along the choice border (**Figure 19B**), showing a more flattened curve (growth rate= 0.34), compared to the choice period (growth rate= 2.26). This could be attributable to the large variability in the inflection points of the individual tuning curves (**Figure 17E**). It is also important to note that the inflection point of the mnemonic curve was found within the choice border only during the choice period (**Table 3**). Taken together, at the population level, our findings suggest that the firing characteristics of P-cells and M-cells are optimized for the perceptual coding of a feature-ambiguous object and the subsequent associative recognition of the object, respectively.

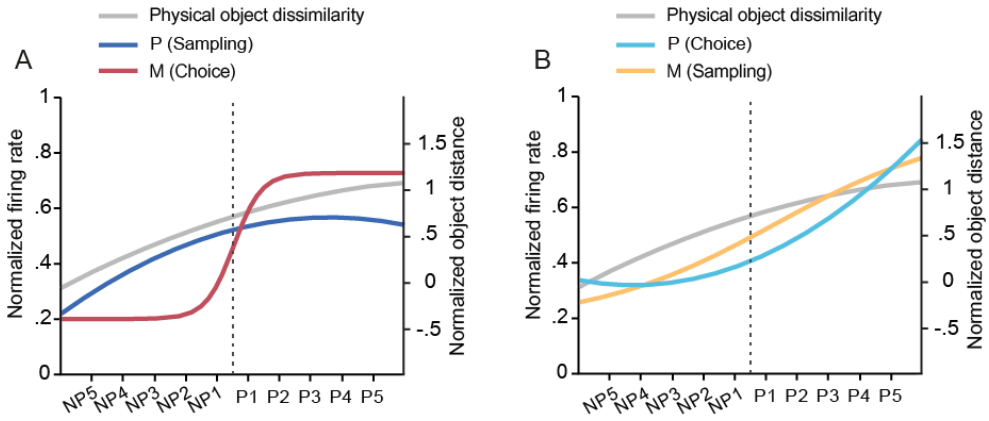

Figure 19. Population object-tuning curves of P-cells and M-cells. (**A**) The population tuning curves of P-cells (P, blue) and M-cells (M, red) from task demand-relevant periods (i.e., object-sampling and choice periods). The curve representing the physical object similarity (gray) was overlaid. (**B**) The population tuning curves of P-cells (cyan) and M-cells (orange) obtained from the event periods that might not be optimal for task demands (i.e., P-cells in the choice period and M-cells in the sampling period).

Table 3. Coefficients for population tuning curves of M-cells fitted by sigmoidal models

Event Period	Performance	Growth Rate	Inflection Point	Lower Asymptote	Upper Asymptote	FR contrast
Sampling Period	Correct	.34	6.32	.19	.90	.71
	Incorrect	2.01	6.35	.36	.52	.16
Choice Period	Correct	2.26	5.53	.20	.83	.63
	Incorrect	.67	5.69	.23	.65	.42

I also examined how the differences in firing characteristics of neurons between correct and incorrect trials (**Figure 17**) influenced the object-tuning curves at the population level. I found that the differences in tuning curves between correct and error trials were more readily observable for M-cells than for P-cells at the population level (**Figure 20**). When a two-way ANOVA was run on the slope of the sigmoidal tuning curve of the population of M-cells, a significant interaction was found between object and correctness in the choice period ($F_{(9,582)}$= 2.32, P< 0.05), but not in the sampling period ($F_{(9,275)}$= 0.84, P= 0.58). This suggests that the representations of morphed objects in M-cells were more sharply orthogonalized according to behavioral choices in correct trials than in error trials.

Taken together, these results suggest that the neural populations in the PER carry out dual functions associated with different task demands, one being monotonic perceptual discrimination of object features and the other being nonlinear orthogonalization considering object memory-guided choice behavior.

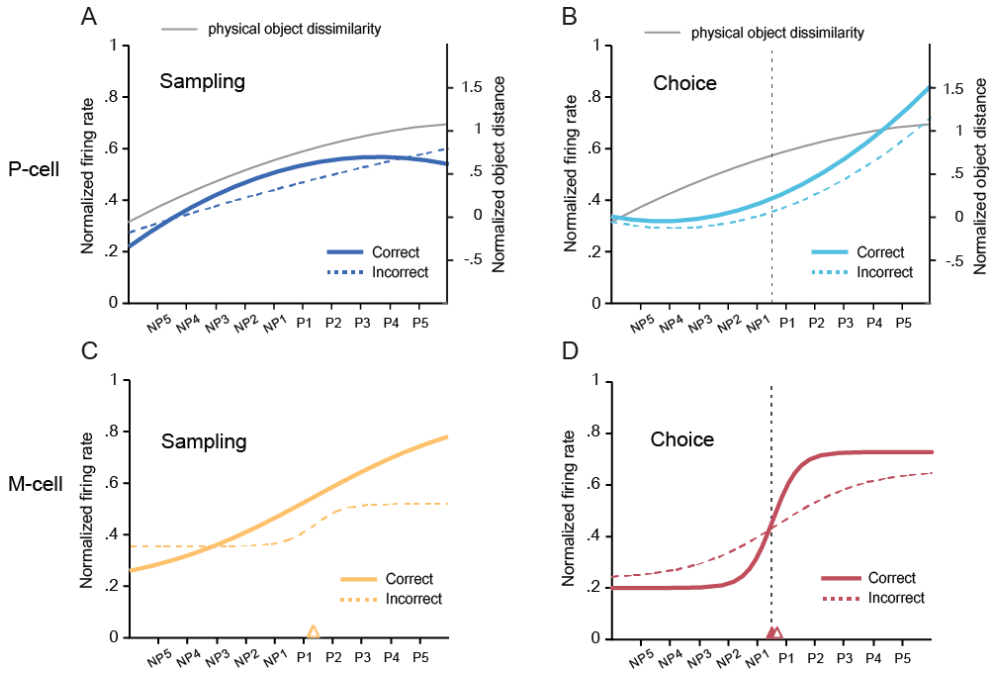

Figure 20. Population object-tuning curves drawn separately for correct and incorrect trials. The tuning curves from incorrect trials (dash) were overlaid on those from correct trials to facilitate comparisons between the two curves according to performance. (**A-B**). For P-cells, the physical object dissimilarity curve (gray dash) was overlaid to show how the perceptual object coding of the P-cells in the sampling (**A**), and choice period (**B**) reflected the physical changes along the morphing dimension. The P-cells in the sampling period (**A**) showed flattened patterns in incorrect trials compared to that in correct trials. The P-cells from both correct and incorrect trials in the choice period (**B**) showed similar fitting patterns with higher growth rate in the preferred category. (**C-D**). For the M-cells, the inflection point of each curve was marked with arrowheads on the abscissa. The filled arrowhead indicates the inflection point of the tuning curve from correct trials, and the empty one from error trials. The vertical dash marks the choice border. The M-cells in the sampling period (**C**) showed non-optimal fitting patterns with the inflection point located off of the choice border both in correct and incorrect trials (**Table 3**). As for the M-cells in the choice period, the inflection points fell within the choice border in both correct and incorrect trials (**Table S1**). However, the contrast in firing rates (the difference between upper and lower asymptote) and growth rate across the choice border Were larger in correct trials than in incorrect trials (**Table S1**).

Mnemonic spiking in the PER guides choice behavior

The results presented so far strongly suggest that the most critical neural correlates of behavioral performance in our task could potentially be found by analyzing the firing characteristics of M-cells during the choice period. Therefore, I examined whether the object information conveyed by M-cells could be decoded directly from the spiking activities of those neurons by using a linear discriminant analysis (**Materials and methods**).

Similar levels of classification performance (i.e., predicting the category of an object based on firing rates) were observed in M-cells between correct and error trials ($t_{(15)}$= 1.0, p= 0.33; paired t-test) in the sampling period (**Figure 21**). However, in the choice period, the classification performance was significantly higher in correct trials than in error trials ($t_{(32)}$= 2.26, p< 0.05; paired t-test)(**Figure 21**), suggesting that M-cells in the choice period conveyed critical object information to guide subsequent choice behavior. These findings further the evidence that the nonlinear, mnemonic response of the neuronal population in the PER is critical for successful performance in the current task.

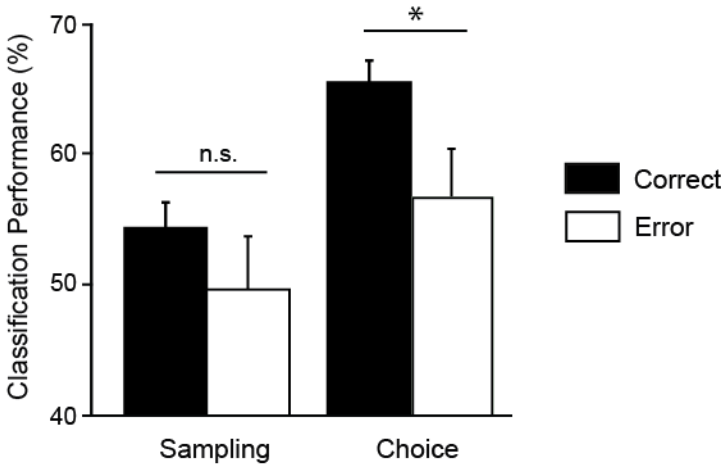

Figure 21. Decoding of object memory based on neural firings of M-cells. Object mnemonic information of the morphed object stimuli was decoded from the spiking information of M-cells in the sampling and choice period. Spiking activity of M-cells carried significantly higher mnemonic information for objects in correct trials than in error trials only in the choice period, but not in the sampling period. *$p < 0.05$.

Discussion

In the current study, morphed object stimuli were used to test rats with perceptually similar, yet different visual stimuli (Clark et al., 2011). Because the morphed objects were associated with one of the two response discs for reward in the task, the rat was required to know the similarities and differences among the objects (i.e., perceptual differences) in the object-sampling period in addition to the paired mnemonic responses (i.e., left or right disc touch) associated with the objects in the choice period. The neuronal population in the PER responded in a task-compatible manner by exhibiting two classes of neurons, P-cells and M-cells. The P-cells exhibited incremental firing patterns, reflecting the physical differences among the morphed objects, whereas the M-cells showed nonlinear response profiles as if to reflect the paired associative relationships between the object stimulus and choice response. I reported in the previous chapter that in the same paradigm, the PER neurons fired differentially according to the choice response associated with the object before and after making a choice response, but not for object identity *per se*. This is mostly likely attributable to the fact that, in my previous study, the object firing rates were obtained from the pre-choice period (from object onset to choice) that did not differentiate between perceptual sampling and choice period. In addition, firing rates for individual objects were averaged for each object category in that study, which may have made it difficult to capture the subtle, yet significant response changes of the PER neurons along the morphing dimension as reported in the current chapter.

The tuning curves of M-cells in the PER obtained at both individual and population levels are reminiscent of the nonlinear changes in neural activity of granule cells of the dentate gyrus (Leutgeb et al., 2005; Leutgeb et al., 2007), and pyramidal cells in CA1 (Wills et al., 2005) of the hippocampus when rats explore continuously morphed geometric environments. The neuronal ensembles in the hippocampus are known to perform putative computations such as “pattern completion” and “pattern separation” for

generalizing similar memory representations into a common representation and orthogonalizing dissimilar memories into separate representations, respectively (Lee et al., 2004; Leutgeb et al., 2005; Leutgeb et al., 2007). A canonical computational theory views pattern separation as an input/output function where the output representation becomes less correlated than its original input signals (O'Reilly and McClelland, 1994; Guzowski et al., 2004). The current results may satisfy this criterion because the neural output (mnemonic tuning curves of M-cells) became more orthogonalized than the original curvilinear inputs (object stimuli varying over the morphing continuum). According to a recently proposed "representational-hierarchical view" of pattern separation (Kent et al., 2016), pattern separation may be present across multiple regions upstream to the hippocampus including the PER, *albeit* to a lesser degree in representational complexity. To the best of my knowledge, the current study provides the first physiological support for this claim that the PER may perform pattern separation (and pattern completion) with respect to object recognition.

However, despite the apparent similarities, there are some notable differences between the present results and the hippocampal literature. One of the main differences is that pattern separation (shown by the mnemonic tuning characteristics) was observable in the PER not only at the neural population level (**Figure 19**), but also at the individual single-unit level (**Figure 15**). This contrasts with the previous hippocampal findings because, to my knowledge, the physiological evidence for pattern separation and pattern completion in the hippocampus has been observable exclusively at the neural population levels (Lee et al., 2004; Leutgeb et al., 2005; Wills et al., 2005; Leutgeb et al., 2007), but not at the individual neuronal level. Another difference is with respect to performance correlates. It is important to note that the putative pattern separation performed by M-cells, especially those from the choice period, contributed to successful behavioral performance in our paradigm. That is, at the individual neuronal level, the M-cells in the choice period exhibited the highest goodness-of-fit to the curve with a more precise point of inflection at the choice border, compared to other conditions. At the population level also, only the M-cells in the choice period showed task-critical tuning profiles with sharper

orthogonalization across the choice border in correct trials, compared to error trials. By contrast, such relationships between neural activity and behavioral performance have been scarcely reported in prior hippocampal studies, possibly due to the fact that most hippocampal data were recorded in a foraging paradigm with no mnemonic requirement to produce choice behavior in response to continuously varying stimuli.

One may argue that the stepwise response profile of M-cells might be derived from a motor response component largely because the objects in the same category were always coupled to a specific choice response. Although it is difficult to rule out such possibility completely, the following aspects of the results make this possibility less likely. First, the parameters used to measure the object-tuning characteristics (e.g., goodness-of-fit and inflection points of the object-turning curve) were significantly disrupted when the rats made errors. If the stepwise responses of M-cells were driven mostly by motor signals associated with touching the left or right disc, such motor components should be also observable in the curve-fitting parameters in error trials because rats made equally decisive motor responses during incorrect trials as they did during correct trials. Second, the object formation carried by the M-cells in the PER was less accurate in error trials in the choice period although the same behavioral responses were made compared to correct trials. Based on these findings, it is likely that the mnemonic firing properties of M-cells in our study were largely driven by the learned associative relationships between the object stimulus categories and choice responses.

Despite the attempt to separate the perceptual and mnemonic components in the task, the two coding schemes might not be strictly discretized because I was able to identify M-cells during the sampling period and P-cells during the choice period, albeit to different degrees. This is plausible in our experimental design because there was no explicit delay to clearly separate the two event periods. It is possible that the choice-related representation of an object might have taken place at the time of object-sampling because the choice response could be specified based on the sample object alone in the current task. Also, there might have been some lingering activities of perceptual signals that persisted through the choice period. Nonetheless, this should not undermine the main

results of the current study because the population of P-cells in the sampling period reflected the physical change along the morphed objects more faithfully than that in the choice period. Likewise, the population of M-cells exhibited sharper and more accurate orthogonalization across the choice border in the choice period than in the sampling period. The perceptual and mnemonic firing correlates of neurons in the PER thus appear to be optimized for information processing required by corresponding task demands associated with object-sampling and behavioral choice in the current task.

The functional heterogeneity of the PER observed in the current study may be linked to its anatomical position as an interface between the MTL memory system and the ventral visual pathway (Bussey and Saksida, 2002; Naya et al., 2003; Murray et al., 2007; Clark et al., 2011; Kravitz et al., 2013). This unique position of the PER may accommodate the presence of these functionally distinct, if not mutually exclusive, classes of neurons, i.e., P-cells and M-cells, in the same area (**Figure 22**).

The present findings provide the first physiological evidence that the rodent PER may serve as a hybrid zone for supporting these dual coding schemes by encoding perceptual differences between objects along the morphing continuum, and also by signaling object recognition signal on the basis of object-associated mnemonic information.

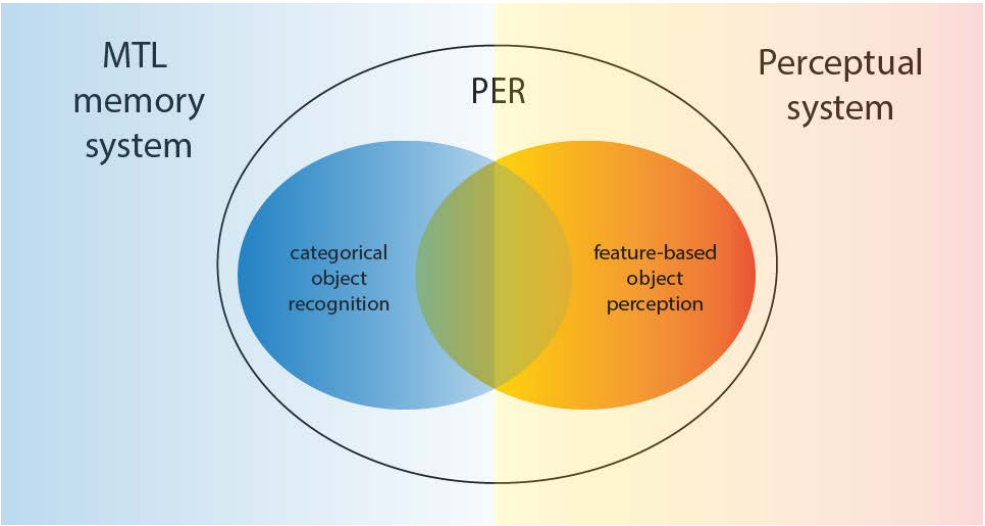

Figure 22. Schematic illustration of the PER as a functional interface between medial temporal lobe memory system and the ventral visual pathway.

General Discussion

In the current thesis, I presented a novel behavioral paradigm designed to investigate visual object information processing in freely-moving rodents. In the task, the rat had to sample a 2D object image on a screen, and had to indicate the memory of the object by choosing one disc images that subsequently appeared in the absence of the object. By temporarily inactivating the PER, I confirmed that the PER is critical for this object memory task. The major advantage of the current paradigm was that I was able to control the onset and offset of the stimulus such that, while the task was self-paced, object sampling took place only in a limited time window. In addition, unlike the previous object paradigms such as DMS/DNMS or SOR, a greater mnemonic demand was placed on the task, since the rats had to learn the paired-associative relationship between an object and target response disc. The design thus precluded the solution of the task merely based on relative familiarity or recency of an object stimulus.

The PER neurons encode the conjunctive relations between an object and response

My initial hypothesis was that the PER neurons would show differential responses patterns toward objects as observed in multiple primate studies (Sakai and Miyashita, 1991; Naya et al., 2001; Naya et al., 2003; Naya and Suzuki, 2011). In the first chapter, I examined the response of PER neurons during the pre-choice period, which was defined from object appearance to the rat making spatial choices. Contrary to my initial expectations, the PER neurons rarely exhibited object-specific neuronal firings, but instead showed differential firing patterns based on the spatial response choices associated with the object.

Previous research on the rodent PER has focused exclusively on its putative role on non-spatial object memory based on the anatomical evidence that the PER forms the nonspatial pathway in the MTL in contrast to the postrhinal cortex (POR), which is part of the spatial pathway (Burwell, 2000; Hargreaves et al., 2005; Eichenbaum and Lipton, 2008; Henriksen et al., 2010). The results of Chapter 1, however, strongly indicate that such dichotomous view of the PER function may be oversimplified since a large proportion of PER neurons encoded a spatial response, or the conjunction of an object and

spatial response, but not the object factor alone. The results are consonant with previous PER recording studies in which PER neurons strongly fired near the spatial locations occupied by objects (Burke et al., 2012; Deshmukh et al., 2012; Burke et al., 2014).

The stronger response-oriented signal observed in the current ask may be driven by the existing, but oft-neglected interconnections between the PER and POR. If that were the case, one would expect to see nonspatial, object-related signals from the POR as well, and this was recently corroborated by Furtak et al. (2012). In the study, they observed that the POR single neurons conveyed strong object signals as well as conjunctive relations between object, place, and context (Furtak et al., 2012). To what extend those two rhinal cortical regions interact with each other to contribute to spatial and nonspatial information processing, however, could only be elucidated by conducting simultaneous neural recordings from two regions, and this remains to be examined in future studies.

The PER encodes object cue-choice outcomes

Another interesting, and yet unexpected finding in the first chapter was that a portion of PER neurons sharply increased their firing rates after behavioral choices were made, and these post-choice responses were synched to the moment of choice rather than to reward delivery. Further analyses revealed that the post-choice neural firings may act as a feedback for the preceding choice response, and the signal acted as a neuronal feedback to subsequently enhance predictability of the choice response in the following trials.

The notion that the PER can be modulated by motivational significance of a cue object such as cue-related outcome, or reward is in fact not new, with several lines of evidence obtained from previous primate studies. Behaviorally, PER-lesioned animals had severe difficulty in maintaining the association between motivational states, and visual cue object that indicated schedules for upcoming reward (Liu et al., 2000). The PER damage also yielded profound deficits in predicting forthcoming reward values based on a visual cue (Clark et al., 2012). At the neuronal level, the response of PER cells signaled upcoming reward schedules as well as the visual cues signaling the reward states (Liu and

Richmond, 2000). Other studies also found that PER neurons represented reward conditions when visual stimuli were associated with either a rewarded or unrewarded outcome states (Mogami and Tanaka, 2006; Ohyama et al., 2012), and PER neurons could convey information about visual cue-outcome contingencies (Eradath et al., 2015), irrespective of reward values. The present results, to my knowledge, is the first demonstration that the rodent PER may serve analogous functions to those identified in primate research.

Multiple brain regions such as the PFC, hippocampus, and orbitofrontal cortex have been implicated as an observer for cue-outcome contingencies (Kepecs et al., 2008; Narayanan and Laubach, 2008; Histed et al., 2009; Wirth et al., 2009; Narayanan et al., 2013). The PER forms reciprocal connections with those regions, and the results suggest that the rodent PER may form a nodal part of the network that monitors choice outcomes to facilitate subsequent cognitive learning.

Overall, the results significantly advance our current understanding of the PER by illustrating that the role of the rodent PER may not limited to the physical aspect of the object memory, but can extend to evaluating cue outcomes or reward values associated with the object. It remains to be further examined, however, that the PER plays such roles specifically when the choice outcome is related to an object stimulus, or can do so regardless of the cue types (e.g., scenes).

The PER neurons encoded the mnemonic and perceptual aspect of an object at both population and single neuronal level

A controversy has been ongoing as to whether the PER is involved primarily in object recognition memory, or whether it also participates in object perception (Bussey et al., 2002; Lee et al., 2005; Murray et al., 2007; Baxter, 2009). To examine this issue, in the current task, rats were initially with two perceptually distinct objects, but later were tested with the ambiguous objects that underwent morphing across 5 levels of ambiguity. In chapter 1, I observed that neuronal responses were modulated by the feature-ambiguity at the population level, but not so much in the single unit levels in the PER. In chapter 2,

I took this issue a step further, and analyzed the data by taking a different analytic approach. Specifically, the pre-choice period defined in Chapter 1 was further separated into two event period, i.e., object sampling period and choice period. When the perceptual demand was higher to differentially encode feature-ambiguous objects in the sampling period, the individual PER neurons gradually adjusted their firing rates as if reflecting the physical changes in the objects along the morphing continuum. However, at the time of decision making after the object disappeared (i.e., in the choice period), the PER neurons adjusted their firing levels nonlinearly according to the task demands associated with the objects (not necessarily reflecting physical features of the object as in the sampling period).

The perceptual-mnemonic hypothesis positions the PER at the boundary between the MTL memory system and the perceptual system extending from the ventral visual stream(Bussey et al., 2005; Murray et al., 2007; Kravitz et al., 2013) . I identified the coexistence of neuronal ensembles showing perceptual and mnemonic response patterns in the PER, and saw that some PER neurons even switched between two response patterns as a function of task events. The results argue against the strict modularization of perception and memory in the PER, and suggest that both components should not be considered independently. It is likely that task-related top-down signals relayed from the higher-order mnemonic areas such as the hippocampus, and the bottom-up signals from the visual sensory corticles come together in the PER to modulate the neuronal activities associated with object information processing in both perceptual and mnemonic domains. The results are also compatible with the neurophysiology in the primate PER where they observed that the perceptual signal for visual stimuli flowed from TE to the PER, whereas the visual-associative memory signal flowed in the backward direction from the PER to TE (Naya et al., 2001). The current results provide the critical evidence by which the two polarized views (i.e., perceptual vs. mnemonic) can be reconciled with the broader notion that the PER may in fact serve dual functions, acting as a functional bridge between perception and memory with respect to object information processing.

Object information is evaluated by integrating concurrent sensory inputs of different modalities. It should be noted that the current thesis dealt exclusively with the object processing in the visual modality domain. However, rats also heavily rely on sniffing or whisking when exploring an object, and it has been shown that the PER damage impairs object identification across various modalities including olfaction (Otto and Eichenbaum, 1992; Feinberg et al., 2012), texture (Buffalo et al., 1999; Ramos, 2014), and audition (Campolattaro and Freeman, 2006; Bang and Brown, 2009). It thus needs to be elucidated in future studies whether the neuronal modulation by visual perceptual ambiguity observed in the current thesis could be extended to other sensory modality domains of an object.

Implications of the current thesis

The current thesis aimed to shed light on multifaceted functional aspects of the PER. For its critical role in object information processing, the PER cortex has been highlighted as the most promising target region for the investigation of life-debilitating cognitive deficits associated with Alzheimer's disease, post-traumatic stress disorder (PTSD), etc. It is hoped that the results from the current thesis lead to the improved understanding of the region, and ultimately contribute to better diagnosis and treatment of such neurological diseases.

Biblography

Aggleton JP, Brown MW (1999) Episodic memory, amnesia, and the hippocampal-anterior thalamic axis. Behav Brain Sci 22:425-444; discussion 444-489.

Aggleton JP, Keen S, Warburton EC, Bussey TJ (1997) Extensive cytotoxic lesions involving both the rhinal cortices and area TE impair recognition but spare spatial alternation in the rat. Brain Res Bull 43:279-287.

Allen TA, Narayanan NS, Kholodar-Smith DB, Zhao Y, Laubach M, Brown TH (2008) Imaging the spread of reversible brain inactivations using fluorescent muscimol. J Neurosci Methods 171:30-38.

Ameen-Ali KE, Easton A, Eacott MJ (2015) Moving beyond standard procedures to assess spontaneous recognition memory. Neurosci Biobehav Rev 53:37-51.

Annese J, Schenker-Ahmed NM, Bartsch H, Maechler P, Sheh C, Thomas N, Kayano J, Ghatan A, Bresler N, Frosch MP, Klaming R, Corkin S (2014) Postmortem examination of patient HM's brain based on histological sectioning and digital 3D reconstruction. Nature Communications 5.

Bang SJ, Brown TH (2009) Perirhinal cortex supports acquired fear of auditory objects. Neurobiol Learn Mem 92:53-62.

Bartho P, Hirase H, Monconduit L, Zugaro M, Harris KD, Buzsaki G (2004) Characterization of neocortical principal cells and interneurons by network interactions and extracellular features. J Neurophysiol 92:600-608.

Bartko SJ, Winters BD, Cowell RA, Saksida LM, Bussey TJ (2007) Perceptual functions of perirhinal cortex in rats: zero-delay object recognition and simultaneous oddity discriminations. J Neurosci 27:2548-2559.

Baxter MG (2009) Involvement of medial temporal lobe structures in memory and perception. Neuron 61:667-677.

Brown MW, Wilson FA, Riches IP (1987) Neuronal evidence that inferomedial temporal cortex is more important than hippocampus in certain processes underlying recognition memory. Brain Res 409:158-162.

Buckley MJ, Gaffan D (1998a) Perirhinal cortex ablation impairs visual object identification. J Neurosci 18:2268-2275.

Buckley MJ, Gaffan D (1998b) Perirhinal cortex ablation impairs configural learning and paired-associate learning equally. Neuropsychologia 36:535-546.

Buckley MJ, Gaffan D (2006) Perirhinal cortical contributions to object perception. Trends Cogn Sci 10:100-107.

Buckley MJ, Booth MC, Rolls ET, Gaffan D (2001) Selective perceptual impairments after perirhinal cortex ablation. J Neurosci 21:9824-9836.

Buffalo EA, Ramus SJ, Clark RE, Teng E, Squire LR, Zola SM (1999) Dissociation between the effects of damage to perirhinal cortex and area TE. Learning & Memory 6:572-599.

Burke SN, Maurer AP, Nematollahi S, Uprety A, Wallace JL, Barnes CA (2014) Advanced age dissociates dual functions of the perirhinal cortex. J Neurosci 34:467-480.

Burke SN, Maurer AP, Hartzell AL, Nematollahi S, Uprety A, Wallace JL, Barnes CA (2012) Representation of three-dimensional objects by the rat perirhinal cortex. Hippocampus 22:2032-2044.

Burwell RD (2000) The parahippocampal region: corticocortical connectivity. Ann N Y Acad Sci 911:25-42.

Burwell RD, Amaral DG (1998) Perirhinal and postrhinal cortices of the rat: interconnectivity and connections with the entorhinal cortex. J Comp Neurol 391:293-321.

Bussey TJ, Saksida LM (2002) The organization of visual object representations: a connectionist model of effects of lesions in perirhinal cortex. Eur. J. Neurosci. 15:355-364.

Bussey TJ, Muir JL, Aggleton JP (1999) Functionally dissociating aspects of event memory: the effects of combined perirhinal and postrhinal cortex lesions on object and place memory in the rat. J Neurosci 19:495-502.

Bussey TJ, Saksida LM, Murray EA (2002) Perirhinal cortex resolves feature ambiguity in complex visual discriminations. Eur. J. Neurosci. 15:365-374.

Bussey TJ, Saksida LM, Murray EA (2005) The perceptual-mnemonic/feature conjunction model of perirhinal cortex function. Q J Exp Psychol B 58:269-282.

Bussey TJ, Saksida LM, Murray EA (2006) Perirhinal cortex and feature-ambiguous discriminations. Learn Mem 13:103-105.

Campolattaro MM, Freeman JH (2006) Perirhinal cortex lesions impair feature-negative discrimination. Neurobiol Learn Mem 86:205-213.

Chudasama Y, Muir JL (1997) A behavioural analysis of the delayed non-matching to position task: the effects of scopolamine, lesions of the fornix and of the prelimbic region on mediating behaviours by rats. Psychopharmacology 134:73-82.

Clark AM, Bouret S, Young AM, Richmond BJ (2012) Intersection of reward and memory in monkey rhinal cortex. J Neurosci 32:6869-6877.

Clark RE, Reinagel P, Broadbent NJ, Flister ED, Squire LR (2011) Intact performance on feature-ambiguous discriminations in rats with lesions of the perirhinal cortex. Neuron 70:132-140.

Cowell RA, Bussey TJ, Saksida LM (2010) Functional Dissociations within the Ventral Object Processing Pathway: Cognitive Modules or a Hierarchical Continuum? Journal of Cognitive Neuroscience 22:2460-2479.

Deshmukh SS, Knierim JJ (2011) Representation of non-spatial and spatial information in the lateral entorhinal cortex. Front Behav Neurosci 5:69.

Deshmukh SS, Johnson JL, Knierim JJ (2012) Perirhinal cortex represents nonspatial, but not spatial, information in rats foraging in the presence of objects: comparison with lateral entorhinal cortex. Hippocampus 22:2045-2058.

Eacott MJ, Gaffan D, Murray EA (1994) Preserved recognition memory for small sets, and impaired stimulus identification for large sets, following rhinal cortex ablations in monkeys. Eur J Neurosci 6:1466-1478.

Eacott MJ, Machin PE, Gaffan EA (2001) Elemental and configural visual discrimination learning following lesions to perirhinal cortex in the rat. Behav Brain Res 124:55-70.

Eichenbaum H, Lipton PA (2008) Towards a functional organization of the medial temporal lobe memory system: role of the parahippocampal and medial entorhinal cortical areas. Hippocampus 18:1314-1324.

Eichenbaum H, Otto T, Cohen NJ (1994) 2 Functional Components of the Hippocampal Memory System. Behavioral and Brain Sciences 17:449-472.

Ennaceur A, Delacour J (1988) A new one-trial test for neurobiological studies of memory in rats. 1: Behavioral data. Behav Brain Res 31:47-59.

Ennaceur A, Aggleton JP (1997) The effects of neurotoxic lesions of the perirhinal cortex combined to fornix transection on object recognition memory in the rat. Behav Brain Res 88:181-193.

Ennaceur A, Neave N, Aggleton JP (1996a) Neurotoxic lesions of the perirhinal cortex do not mimic the behavioural effects of fornix transection in the rat. Behavioural Brain Research 80:9-25.

Ennaceur A, Neave N, Aggleton JP (1996b) Neurotoxic lesions of the perirhinal cortex do not mimic the behavioural effects of fornix transection in the rat. Behav Brain Res 80:9-25.

Eradath MK, Mogami T, Wang G, Tanaka K (2015) Time context of cue-outcome associations represented by neurons in perirhinal cortex. J Neurosci 35:4350-4365.

Fahy FL, Riches IP, Brown MW (1993) Neuronal activity related to visual recognition memory: long-term memory and the encoding of recency and familiarity information in the primate anterior and medial inferior temporal and rhinal cortex. Exp Brain Res 96:457-472.

Feinberg LM, Allen TA, Ly D, Fortin NJ (2012) Recognition memory for social and non-social odors: differential effects of neurotoxic lesions to the hippocampus and perirhinal cortex. Neurobiol Learn Mem 97:7-16.

Furtak SC, Allen TA, Brown TH (2007a) Single-unit firing in rat perirhinal cortex caused by fear conditioning to arbitrary and ecological stimuli. J Neurosci 27:12277-12291.

Furtak SC, Ahmed OJ, Burwell RD (2012) Single neuron activity and theta modulation in postrhinal cortex during visual object discrimination. Neuron 76:976-988.

Furtak SC, Wei SM, Agster KL, Burwell RD (2007b) Functional neuroanatomy of the parahippocampal region in the rat: the perirhinal and postrhinal cortices. Hippocampus 17:709-722.

Gaffan EA, Eacott MJ (1995) A computer-controlled maze environment for testing visual memory in the rat. J Neurosci Methods 60:23-37.

Guzowski JF, Knierim JJ, Moser EI (2004) Ensemble dynamics of hippocampal regions CA3 and CA1. Neuron 44:581-584.

Hargreaves EL, Rao G, Lee I, Knierim JJ (2005) Major dissociation between medial and lateral entorhinal input to dorsal hippocampus. Science 308:1792-1794.

Harris KD, Hirase H, Leinekugel X, Henze DA, Buzsaki G (2001) Temporal interaction between single spikes and complex spike bursts in hippocampal pyramidal cells. Neuron 32:141-149.

Henriksen EJ, Colgin LL, Barnes CA, Witter MP, Moser MB, Moser EI (2010) Spatial representation along the proximodistal axis of CA1. Neuron 68:127-137.

Herremans AHJ, Hijzen TH, Slangen JL (1995) The Object Delayed-Nonmatching-to-Sample Task in Rats Does Not Depend on Working-Memory. Neuroreport 6:1963-1965.

Histed MH, Pasupathy A, Miller EK (2009) Learning substrates in the primate prefrontal cortex and striatum: sustained activity related to successful actions. Neuron 63:244-253.

Kajiwara R, Takashima I, Mimura Y, Witter MP, Iijima T (2003) Amygdala input promotes spread of excitatory neural activity from perirhinal cortex to the entorhinal-hippocampal circuit. J Neurophysiol 89:2176-2184.

Kealy J, Commins S (2011) The rat perirhinal cortex: A review of anatomy, physiology, plasticity, and function. Prog Neurobiol 93:522-548.

Kent BA, Hvoslef-Eide M, Saksida LM, Bussey TJ (2016) The representational-hierarchical view of pattern separation: Not just hippocampus, not just space, not just memory? Neurobiol Learn Mem.

Kepecs A, Uchida N, Zariwala HA, Mainen ZF (2008) Neural correlates, computation and behavioural impact of decision confidence. Nature 455:227-231.

Kim J, Delcasso S, Lee I (2011) Neural correlates of object-in-place learning in hippocampus and prefrontal cortex. J Neurosci 31:16991-17006.

Kravitz DJ, Saleem KS, Baker CI, Ungerleider LG, Mishkin M (2013) The ventral visual pathway: an expanded neural framework for the processing of object quality. Trends Cogn Sci 17:26-49.

Lee AC, Bussey TJ, Murray EA, Saksida LM, Epstein RA, Kapur N, Hodges JR, Graham KS (2005) Perceptual deficits in amnesia: challenging the medial temporal lobe 'mnemonic' view. Neuropsychologia 43:1-11.

Lee I, Yoganarasimha D, Rao G, Knierim JJ (2004) Comparison of population coherence of place cells in hippocampal subfields CA1 and CA3. Nature 430:456-459.

Leutgeb JK, Leutgeb S, Moser MB, Moser EI (2007) Pattern separation in the dentate gyrus and CA3 of the hippocampus. Science 315:961-966.

Leutgeb JK, Leutgeb S, Treves A, Meyer R, Barnes CA, McNaughton BL, Moser MB, Moser EI (2005) Progressive transformation of hippocampal neuronal representations in "morphed" environments. Neuron 48:345-358.

Li SM, Cullen WK, Anwyl R, Rowan MJ (2003) Dopamine-dependent facilitation of LTP induction in hippocampal CA1 by exposure to spatial novelty. Nature Neuroscience 6:526-531.

Liu P, Bilkey DK (1998) Excitotoxic lesions centered on perirhinal cortex produce delay-dependent deficits in a test of spatial memory. Behav Neurosci 112:512-524.

Liu Z, Richmond BJ (2000) Response differences in monkey TE and perirhinal cortex: stimulus association related to reward schedules. J Neurophysiol 83:1677-1692.

Liu Z, Murray EA, Richmond BJ (2000) Learning motivational significance of visual cues for reward schedules requires rhinal cortex. Nat Neurosci 3:1307-1315.

McTighe SM, Cowell RA, Winters BD, Bussey TJ, Saksida LM (2010) Paradoxical false memory for objects after brain damage. Science 330:1408-1410.

Meunier M, Bachevalier J, Mishkin M, Murray EA (1993) Effects on visual recognition of combined and separate ablations of the entorhinal and perirhinal cortex in rhesus monkeys. J. Neurosci 13:5418-5432.

Miller EK, Li L, Desimone R (1991) A neural mechanism for working and recognition memory in inferior temporal cortex. Science 254:1377-1379.

Miyashita Y, Chang HS (1988) Neuronal correlate of pictorial short-term memory in the primate temporal cortex. Nature 331:68-70.

Mogami T, Tanaka K (2006) Reward association affects neuronal responses to visual stimuli in macaque te and perirhinal cortices. J Neurosci 26:6761-6770.

Mumby DG, Pinel JP (1994) Rhinal cortex lesions and object recognition in rats. Behav Neurosci 108:11-18.

Mumby DG, Pinel JPJ, Wood ER (1990) Nonrecurring-Items Delayed Nonmatching-to-Sample in Rats - a New Paradigm for Testing Nonspatial Working Memory. Psychobiology 18:321-326.

Murray EA, Bussey TJ, Saksida LM (2007) Visual perception and memory: a new view of medial temporal lobe function in primates and rodents. Annu Rev Neurosci 30:99-122.

Murty VP, LaBar KS, Adcock RA (2012) Threat of Punishment Motivates Memory Encoding via Amygdala, Not Midbrain, Interactions with the Medial Temporal Lobe. Journal of Neuroscience 32:8969-8976.

Narayanan NS, Laubach M (2008) Neuronal correlates of post-error slowing in the rat dorsomedial prefrontal cortex. J Neurophysiol 100:520-525.

Narayanan NS, Cavanagh JF, Frank MJ, Laubach M (2013) Common medial frontal mechanisms of adaptive control in humans and rodents. Nat Neurosci 16:1888-1895.

Naya Y, Suzuki WA (2011) Integrating What and When Across the Primate Medial Temporal Lobe. Science 333:773-776.

Naya Y, Yoshida M, Miyashita Y (2001) Backward spreading of memory-retrieval signal in the primate temporal cortex. Science 291:661-664.

Naya Y, Yoshida M, Miyashita Y (2003) Forward Processing of Long-Term Associative Memory in Monkey Inferotemporal Cortex. J. Neurosci. 23:2861-2871.

Norman G, Eacott MJ (2004) Impaired object recognition with increasing levels of feature ambiguity in rats with perirhinal cortex lesions. Behavioural Brain Research 148:79-91.

Norman G, Eacott MJ (2005) Dissociable effects of lesions to the perirhinal cortex and the postrhinal cortex on memory for context and objects in rats. Behav Neurosci 119:557-566.

O'Reilly RC, McClelland JL (1994) Hippocampal conjunctive encoding, storage, and recall: avoiding a trade-off. Hippocampus 4:661-682.

Ohyama K, Sugase-Miyamoto Y, Matsumoto N, Shidara M, Sato C (2012) Stimulus-related activity during conditional associations in monkey perirhinal cortex neurons depends on upcoming reward outcome. J Neurosci 32:17407-17419.

Otto T, Eichenbaum H (1992) Complementary roles of the orbital prefrontal cortex and the perirhinal-entorhinal cortices in an odor-guided delayed-nonmatching-to-sample task. Behav Neurosci 106:762-775.

Paxinos G, Watson C (2007) The rat brain in stereotaxic coordinates, Ed 6. Amsterdam: Academic/Elsevier.

Paz R, Pelletier JG, Bauer EP, Pare D (2006) Emotional enhancement of memory via amygdala-driven facilitation of rhinal interactions. Nat Neurosci 9:1321-1329.

Perugini A, Laing M, Berretta N, Aicardi G, Bashir ZI (2012) Synaptic plasticity from amygdala to perirhinal cortex: a possible mechanism for emotional enhancement of visual recognition memory? Eur J Neurosci 36:2421-2427.

Pitkanen A, Pikkarainen M, Nurminen N, Ylinen A (2000) Reciprocal connections between the amygdala and the hippocampal formation, perirhinal cortex, and postrhinal cortex in rat - A review. Parahippocampal Region 911:369-391.

Ramos JM (2014) Essential role of the perirhinal cortex in complex tactual discrimination tasks in rats. Cereb Cortex 24:2068-2080.

Sakai K, Miyashita Y (1991) Neural organization for the long-term memory of paired associates. Nature 354:152-155.

Schmitzer-Torbert N, Jackson J, Henze D, Harris K, Redish AD (2005) Quantitative measures of cluster quality for use in extracellular recordings. Neuroscience 131:1-11.

Schoenbaum G, Chiba AA, Gallagher M (1998) Orbitofrontal cortex and basolateral amygdala encode expected outcomes during learning. Nat Neurosci 1:155-159.

Schultz W (1998) Predictive reward signal of dopamine neurons. J Neurophysiol 80:1-27.

Schultz W, Apicella P, Ljungberg T (1993) Responses of Monkey Dopamine Neurons to Reward and Conditioned-Stimuli during Successive Steps of Learning a Delayed-Response Task. Journal of Neuroscience 13:900-913.

Scoville WB, Milner B (1957) Loss of recent memory after bilateral hippocampal lesions. J Neurol Neurosurg Psychiatry 20:11-21.

Snow JC, Pettypiece CE, McAdam TD, McLean AD, Stroman PW, Goodale MA, Culham JC (2011) Bringing the real world into the fMRI scanner: Repetition effects for pictures versus real objects. Sci Rep 1.

Squire LR, Zola-Morgan S (1991) The medial temporal lobe memory system. Science 253:1380-1386.

Suzuki WA (2009) Perception and the medial temporal lobe: evaluating the current evidence. Neuron 61:657-666.

Suzuki WA, Baxter MG (2009) Memory, Perception, and the Medial Temporal Lobe: A Synthesis of Opinions. Neuron 61:678-679.

Suzuki WA, Zola-Morgan S, Squire LR, Amaral DG (1993) Lesions of the perirhinal and parahippocampal cortices in the monkey produce long-lasting memory impairment in the visual and tactual modalities. J Neurosci 13:2430-2451.

Van Hoesen GW, Yeterian EH, Lavizzo-Mourey R (1981) Widespread corticostriate projections from temporal cortex of the rhesus monkey. J Comp Neurol 199:205-219.

Wills TJ, Lever C, Cacucci F, Burgess N, O'Keefe J (2005) Attractor dynamics in the hippocampal representation of the local environment. Science 308:873-876.

Winters BD, Bussey TJ (2005) Glutamate Receptors in Perirhinal Cortex Mediate Encoding, Retrieval, and Consolidation of Object Recognition Memory. J. Neurosci. 25:4243-4251.

Winters BD, Forwood SE, Cowell RA, Saksida LM, Bussey TJ (2004) Double dissociation between the effects of peri-postrhinal cortex and hippocampal lesions on tests of object recognition and spatial memory: heterogeneity of function within the temporal lobe. J Neurosci 24:5901-5908.

Wirth S, Avsar E, Chiu CC, Sharma V, Smith AC, Brown E, Suzuki WA (2009) Trial outcome and associative learning signals in the monkey hippocampus. Neuron 61:930-940.

Xiang JZ, Brown MW (1998) Differential neuronal encoding of novelty, familiarity and recency in regions of the anterior temporal lobe. Neuropharmacology 37:657-676.

Zhu XO, Brown MW, Aggleton JP (1995) Neuronal signalling of information important to visual recognition memory in rat rhinal and neighbouring cortices. Eur J Neurosci 7:753-765.

국문초록

사물기억과 지각에 대한 후각주위피질의 역할

안재롱

인간을 포함한 동물을은 환경속에서 물체와 같은 결정적인 자극에 기반하여 어디로 가야할지 등의 행동을 정하며, 심지어 그 자극이 없는 상황에서도 자극에 대한 기억을 바탕으로 행동을 결정한다. 이처럼 자극을 처리하고 인지하여 미래의 행동을 결정하는 능력은 개체의 생존에 있어 매우 결정적이다. 스코빌과 밀너가 처음 보고한 기억상실증 환자 H.M.은 측두영의 손상을 입은 후 심각한 인지기억 능력의 장애를 보였는데, 이후 뇌의 후각주위피질은 사물인식기억을 관장하는 뇌의 중요한 영역중 하나로 널리 연구되었다.

후각주위피질의 역할에 관해서 신경과학계에는 그동안 두가지의 가설이 지배적이었다. 첫번째 가설은 후각주위피질이 물체인식기억에 중요하다는 것인 데, 이는 환자나 동물 실험에서 오랫동안 밝혀져 왔다. 두번째 가설은 비교적 최근에 제기되었는데, 후각주위피질이 물체인식과 관련된 기억 뿐 아니라, 많은 시각적 특징을 공유하여 시각적으로 모호한 물체들을 지각적으로 구분하는데도 중요하다는 것이다.

후각주위피질의 기능적 역할은 주로 동물실험을 통해서 연구되어 왔는데, 이런 연구들에 따르면 후각주위피질에 손상을 입은 동물들은 행동적으로 물체를 인식하는데 어려움을 겪었다. 좀 더 직접적인 증거는

신경세포의 신호를 측정해서 얻을 수 있을텐데, 지금까지 후각주위피질의 세포에서 사물정보와 관련된 신경적 활성화를 찾으려는 생리학적 연구는 드물었다. 또한 그런 생리학적 연구는 몸의 움직임이 극도로 제한된 동물들에게서 이루어졌고, 물체를 제외하고도 여러 요소들이 혼재된 과제를 사용했기 때문에 세포의 발화를 물체자극과 직접적으로 상관짓기에 어려움이 있었다.

이 논문은 이 분야에서 수십년간 부족했던 생리학적 증거를 제시하는데 초점을 맞추고 있다. 논문에서 본 저자는 설치류 후각주위피질의 물체정보처리 과정과 관련된 주요 논제들을 다루기 위해 고안된 새로운 물체기억과제를 제시할 것이다. 후각주위피질과 관련된 기존의 해부학적, 행동적 발견들에 근거하여 본 저자는 첫번째로 설치류 후각주위피질의 신경세포들이 물체자극의 정체에 따라 다른 발화패턴을 보이는지를 측정했다. 두번째로는 후각주위피질 신경세포의 발화가 모호한 시각적 특성을 갖는 물체의 지각적 특성에 반응하는지를 살펴보았다.